



UNIVERSITY OF CRETE
INTERDISCIPLINARY GRADUATE
PROGRAM
OPTICS&VISION



MSc dissertation

**«Distributions of axial length and refractive
error in patients with keratoconus»**

Papadogiannis Petros



Supervisors:

1. Plainis Sotiris
2. Panagopoulou Sofia
3. Kimionis Giorgos

Heraklion 2016

This study was submitted as part of the obligations for the conferment of the Master in Science certification of the MSc Program “Optics and Vision” and was presented at the three-member committee constituted by:

- 1. Tsilimbaris M., Professor**
- 2. Kymionis G., Assistant Professor**
- 3. Detorakis E., Assistant Professor**

ABSTRACT

Purpose: The research aims, through a cross-sectional study in patients with keratoconus, to check whether the balance between axial length-corneal power is disrupted, and show us if a keratoconic eye is relatively "large" or not, which could assess the development risk factor of keratoconus. Also, by evaluating the binocular differences in a group of children / young people, who usually have keratoconus in different stages in both eyes, it will be checked whether these certain differences are connected with any difference in axial length.

Patients and Methods: This study involved 163 keratoconic patients and 175 emmetropes. Both eyes' data were recorded. These data were: a) the refraction of the eye which was taken by an automatic refractometer firstly, and by subjective refraction secondly b) the curvature of the cornea via corneal topography by Galilei c) the axial length and the anterior chamber depth of the eye using the IOL Master biometric system. The eyes of each subject were grouped based on keratoconus progress, in more progressed and less progressed keratoconus. The criteria were the astigmatism and the corneal radius. Statistical analysis was performed among the three groups: less progressed keratoconic eyes, more progressed keratoconic eyes and emmetropes.

Results: The axial length found to have no significant difference between less and more progressed eyes, but the sphere and the cylinder differ significantly and are affected by the lower values in corneal radius (steeper cornea) because of the ectasia in more progressed eyes. The mean values for anterior chamber depth in less and more progressed keratoconus are 3.68mm and 3.74mm respectively, thus more progressed keratoconic eyes have longer anterior chamber depth. That difference though, does not affect the axial length.

The keratoconic eyes found to be more myopic (longer) compared to the emmetropic group, and as expected, keratoconic corneas are much steeper than the emmetropic.

Conclusion: The more progressed keratoconic eyes are more myopic but not longer (at a level that explains the difference of myopia) than the less progressed. Thus, the ectasia caused by keratoconus is the factor that affects the refractive profile in patients with keratoconus.

ΠΕΡΙΛΗΨΗ

Σκοπός: Η έρευνα που θα διεξαχθεί έχει ως σκοπό,μέσω μίας cross-sectional μελέτης σε ασθενείς με κερατόκωνο,να γίνει έλεγχος του κατά πόσο διαταράσσεται η ισορροπία αξονικού μήκους-κερατοειδικής ισχύος και να μας δείξει αν ένας κερατοκωνικός οφθαλμός είναι σχετικά «μεγάλος» ή το αντίθετο,κάτι που θα μπορούσε να εκτιμήσει τον παράγοντα κινδύνου εξέλιξης κερατόκωνου.Επιπλέον,μέσω της αξιολόγησης των διοφθάλμιων διαφορών σε μια ομάδα παιδιών/νεαρών ατόμων,που συνήθως εμφανίζουν κερατόκωνο σε διαφορετικά στάδια στα δύο μάτια,θα γίνει έλεγχος αν οι συγκεκριμένες διαφορές είναι συνδεδεμένες με όποια διαφορά στο αξονικό μήκος.

Ασθενείς και Μεθοδολογία: Σε αυτή την έρευνα πήραν μέρος 163 ασθενείς με κερατόκωνο και 175 εμμέτροπες.Καταγράφηκαν δεδομένα και των δύο οφθαλμών τους. Τα δεδομένα αυτά είναι α)η διάθλαση του οφθαλμού η οποία αρχικά πάρθηκε με αυτόματο διαθλασίμετρο,και με υποκειμενική διάθλαση στη συνέχεια β)η καμπυλότητα του κερατοειδούς η οποία πάρθηκε μέσω τοπογραφίας κερατοειδούς με τον τοπογράφο του κερατοειδούς Galilei και γ) το αξονικό μήκος και το βάθος προσθίου θαλάμου του οφθαλμού τα οποία πάρθηκαν με τη χρήση του IOL Master. Οι οφθαλμοί κάθε υποκειμένου διαχωρίστηκαν με βάση την πρόοδο του κερατόκωνου σε περισσότερο προχωρημένο και σε λιγότερο προχωρημένο κερατόκωνο. Τα κριτήρια διαχωρισμού ήταν ο αστιγματισμός και οι ακτίνα καμπυλότητας του κερατοειδούς. Τέλος,ακολούθησε στατιστική ανάλυση των δεδομένων των τριών ομάδων(περισσότερο προχωρημένοι κερατοκωνικοί οφθαλμοί,λιγότερο προχωρημένοι κερατοκωνικοί οφθαλμοί,εμμέτροπικοί οφθαλμοί).

Αποτελέσματα: Το αξονικό μήκος βρέθηκε να μην έχει σημαντική διαφορά ανάμεσα στους λιγότερο και τους περισσότερο προχωρημένους κερατόκωνους,αλλά το σφέρωμα και ο κύλινδρος διαφέρουν σημαντικά, και επηρεάζονται από τις χαμηλότερες τιμές της ακτίνας καμπυλότητας λόγω μεγαλύτερης εκτασίας στους περισσότερο προχωρημένους κερατόκωνους. Οι μέσες τιμές του βάθους προσθίου θαλάμου σε λιγότερο και περισσότερο προχωρημένους κερατόκωνους είναι 3,68χιλιοστα και 3,74χιλιοστα αντίστοιχα. Άρα,οι οφθαλμοί με προχωρημένο κερατόκωνο έχουν μεγαλύτερο βάθος προσθίου θαλάμου. Τα κερατοκωνικά μάτια βρέθηκαν να είναι περισσότερο μυωπικά (μακρύτερα) σε σύγκριση με την ομάδα των εμμετρόπων, και όπως περιμέναμε,οι κερατοειδείς με κερατόκωνο παρουσιάζουν μεγαλύτερη κυρτότητα από τους εμμετροπικούς.

Συμπεράσματα: Οι οφθαλμοί με περισσότερο προχωρημένο κερατόκωνο είναι πιο μυωπικοί, όχι όμως και μακρύτεροι(σε επίπεδο που να δικαιολογεί τη διαφορά της μυωπίας) από τους οφθαλμούς με λιγότερο προχωρημένο κερατόκωνο. Άρα, η εκτασία που προκαλείται από τον κερατόκωνο επηρεάζει το διαθλαστικό προφίλ στους ασθενείς με κερατόκωνο.

CONTENTS

PART 1

1) Introduction

1.1 Vision	9
1.1.2 Anatomy of the eye.....	9
1.2 Refractive errors.....	12
1.2.1 emmetropia.....	12
1.2.2 ametropia.....	13
1.2.3 myopia.....	13
1.2.4 hyperopia.....	14
1.2.5 astigmatism.....	15
1.3 Age and refractive errors.....	15
1.3.1 emmetropization.....	18
1.4 Distribution of myopia in population.....	20
1.4.1 ASIA.....	21
1.4.2 EUROPE.....	22
1.4.3 NORTH AMERICA (UNITED STATES).....	23
1.4.4 AUSTRALIA.....	23
1.4.5 SOUTH AMERICA (BRAZIL).....	23

2) KERATOCONUS

2.1 Definition.....	25
2.2 Prevalence, distribution and course	26
2.3 Associated disease.....	26
2.3.1 Systemic disease.....	26
2.3.2 Ocular disease.....	27
2.4 What causes Keratoconus?.....	28
2.4.1 Genetic Causes.....	28
2.4.2 Environmental Causes.....	28
2.4.3 Hormonal causes.....	28
2.5 Keratoconus symptoms and signs.....	29
2.5.1 Symptoms.....	29
2.5.2 Signs.....	29
2.6 Classification.....	31

2.7 Diagnostic procedures.....	31
2.8 Optical performance and keratoconus (influence).....	32
2.9 Management and treatment of keratoconus.....	32
2.10 Aim of the study.....	37

PART 2

3) METHODS

3.1 Subjective refraction.....	38
3.2 Refractometer.....	39
3.2.1 Automatic refractometers.....	39
3.2.2 Canon RK_F1 automatic refractometer.....	40
3.3 IOL MASTER ZEISS.....	41
3.3.1 Axial length measurements.....	41
3.3.2 Measurement of anterior chamber depth (ACD).....	43
3.3.3 Keratometry.....	45
3.4 The GALILEI™ Dual Scheimpflug Analyzer.....	46
3.4.1 Dual Scheimpflug Imaging.....	46
3.4.2 Rotational Scanning.....	48
3.4.3 The GALILEI™ Software Interface.....	48
3.4.4 Advantages of the GALILEI™ System’s Dual Scheimpflug Imaging.....	51

PART 3

4) STATISTICAL ANALYSIS

4.1 First part (31 patients’ data).....	52
4.1.1 More progressed eyes vs less progressed eyes.....	53
4.1.2 Axial length (more progressed eyes vs less progressed eyes).....	53
4.1.3 Corneal radius (more progressed eyes vs less progressed eyes).....	54
4.1.4 Axial length vs corneal radius.....	55
4.2 Second part (combined data-163 patients).....	56
4.2.1 Normality tests.....	56
4.2.2 Distributions.....	57
4.2.3 Axial length (more progressed eyes vs less progressed eyes).....	59

4.2.4 Sphere (more progressed eyes vs less progressed eyes).....	60
4.2.5 Cylinder (more progressed eyes vs less progressed eyes).....	62
4.2.6 Corneal radius (more progressed eyes vs less progressed eyes).....	63
4.2.7 Anterior chamber depth (more progressed eyes vs less progressed eyes).....	64
4.2.8 Corneal radius/axial length (more progressed eyes vs less progressed eyes).....	65
4.2.9 Axial length vs sphere.....	66
4.2.10 Sphere vs corneal radius.....	67
4.2.11 Axial length vs anterior chamber depth.....	68
4.2.12 Difference in axial length between more and less progressed eyes.....	69
vs Difference in anterior chamber depth between more and less progressed eyes	
4.2.13 Corneal radius vs anterior chamber depth.....	70
4.2.14 Difference in corneal radius between more and less progressed eyes.....	71
vs Difference in anterior chamber depth between more and less progressed eyes	
4.2.15 Corneal radius vs axial length.....	72

5) DISCUSSION

5.1 Normality tests and distributions in emmetropic group.....	73
5.1.2 Axial length comparison (keratoconic patients vs emmetropes).....	74
5.1.3 Corneal radius comparison (keratoconic patients vs emmetropes).....	75
5.1.4 Corneal radius/axial length comparison (keratoconic patients vs emmetropes).....	76

5.2 Conclusion.....	77
---------------------	----

6) REFERENCES.....	78
--------------------	----

PART 1

1)Introduction

1.1 Vision

Vision is by far the most used of the five senses and is one of the primary means that we use to gather information from our surroundings. More than 75% of the information we receive about the world around us consists of visual information.

Vision occurs when light enters the eye through the pupil. With help from other important structures in the eye, like the iris and cornea, the appropriate amount of light is directed towards the lens.

Just like a lens in a camera sends a message to produce a film, the lens in the eye 'refracts' (bends) incoming light onto the retina. The retina is made up by millions of specialized cells known as rods and cones, which work together to transform the image into electrical energy, which is sent to the optic disk on the retina and transferred via electrical impulses along the optic nerve to be processed by the brain.

1.1.2 Anatomy of the eye

What makes up an eye (fig.1)

- **Iris:** regulates the amount of light that enters your eye. It forms the colored, visible part of your eye in front of the lens. Light enters through a central opening called the pupil.
- **Pupil:** the circular opening in the center of the iris through which light passes into the lens of the eye. The iris controls widening and narrowing (dilation and constriction) of the pupil.
- **Cornea:** the transparent circular part of the front of the eyeball. It refracts the light entering the eye onto the lens, which then focuses it onto the retina. The cornea contains no blood vessels and is extremely sensitive to pain.
- **Lens:** a transparent structure situated behind your pupil. It is enclosed in a thin transparent capsule and helps to refract incoming light and focus it onto the retina. A

cataract is when the lens becomes cloudy, and a cataract operation involves the replacement of the cloudy lens with an artificial plastic lens.

- **Choroid:** the middle layer of the eye between the retina and the sclera. It also contains a pigment that absorbs excess light so preventing blurring of vision.
- **Ciliary body:** the part of the eye that connects the choroid to the iris.
- **Retina:** a light sensitive layer that lines the interior of the eye. It is composed of light sensitive cells known as rods and cones. The human eye contains about 125 million rods, which are necessary for seeing in dim light. Cones, on the other hand, function best in bright light. There are between 6 and 7 million cones in the eye and they are essential for receiving a sharp accurate image and for distinguishing colors. The retina works much in the same way as film in a camera.
- **Macula:** a yellow spot on the retina at the back of the eye which surrounds the fovea.
- **Fovea:** forms a small indentation at the center of the macula and is the area with the greatest concentration of cone cells. When the eye is directed at an object, the part of the image that is focused on the fovea is the image most accurately registered by the brain.
- **Optic disc:** the visible (when the eye is examined) portion of the optic nerve, also found on the retina. The optic disc identifies the start of the optic nerve where messages from cone and rod cells leave the eye via nerve fibers to the optic center of the brain. This area is also known as the 'blind spot'.
- **Optic nerve:** leaves the eye at the optic disc and transfers all the visual information to the brain.
- **Sclera:** the white part of the eye, a tough covering with which the cornea forms the external protective coat of the eye.
- **Rod cells** are one of the two types of light-sensitive cells in the retina of the eye. There are about 125 million rods, which are necessary for seeing in dim light.

- **Cone cells** are the second type of light sensitive cells in the retina of the eye. The human retina contains between six and seven million cones; they function best in bright light and are essential for acute vision (receiving a sharp accurate image). It is thought that there are three types of cones, each sensitive to the wavelength of a different primary color – red, green or blue. Other colors are seen as combinations of these primary colors.

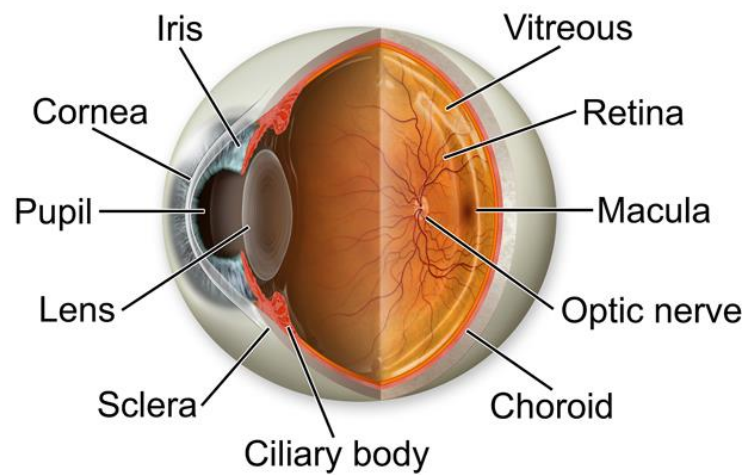


Fig.1. Eye's anatomy

1.2 Refractive errors

1.2.1 Emmetropia

When the eye focuses on an object of interest (a parallel ray beam enters in the eye), the image of the object is focused clearly on the retina, and more specific on the fovea. (fig.2)

The eye is not a static organ and this is why an object can be focused clear on the retina within a range of distances.

The closest distance that an object can be focused clearly is called the near point and the furthest is called the far point of the eye.

In Emmetropia eye the far point is to infinity.

The difference between the near and the far point is called adjustment range and is the area in which objects can be focused clearly on the retina. If the adjustment range is not appropriate, the objects of interest cannot be formed clearly on the retina. In this case, the retinal image is blurred, and this reduces the visual acuity of the eye. The calculation of the adjustment (in diopters) which is needed for sharp vision in a certain distance equals to the inverse of this distance.

e.g. for 2m distance ,is required $1/2D$ of adjustment .

The ciliary body is attached to the lens by connective tissue called the zonular fibers (fibers of Zinn) and is responsible for the mechanism of adjustment.

Relaxation of the ciliary muscle puts tension on these fibers and changes the shape of the lens. The lens thickness is reduced, thereby improving the focus on distant objects (far point). When the muscle contracts, the curvature and thickness of the lens increases, so the eye focuses better to nearby objects (near point).

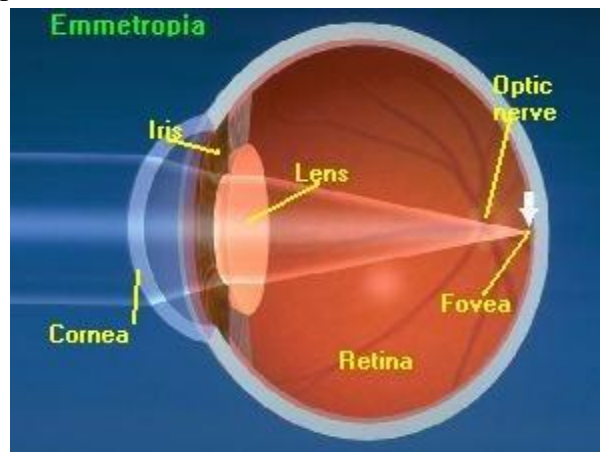


Fig.2 Emmetropia

1.2.2 Ametropia

An eye is called ametropic, when its far point is not to infinity. When the incident ray beam focuses ahead or behind the retina, the image of the object is not clear and the situation called ametropia.

1.2.3 Myopia

The myopic refractive error occurs when the far point is at a finite distance ahead of the eye, and the incident beam of rays is focused in front of the retina. (fig.3)

The distance of the far point from the cornea (in meters) and the degree of ametropia (in diopters) are connected with a reverse relation.

e.g. the far point of an eye with -5D is $1/5 = 0,20\text{m}$ front of the cornea.

There are two types of myopia:

Refractive myopia: Due to great refractive power of the eye, because of greater curvature of the cornea, or by increasing the refractivity of the lens.

Axial myopia: Due to great axial length of the eye.

This distinction is not always secure, since there are emmetropic eyes with great refractive power or large axial length. However, if in an emmetropic eye the axial length will increase, then the eye becomes myopic according to the following formula:

$$\delta L \approx -\delta l * F^2 / n$$

where δL is the refractive error because of the change in the axial length, F the total eye power ($\sim 60\text{ D}$) and n the refractive index of the vitreous body. Similarly if in an emmetropic eye the cornea becomes more curved, which happens mainly due to the decrease of the radius of curvature of the anterior surface of the cornea, the eye becomes myopic under the following formula:

$$F_c = (n-1) / r \quad (2)$$

where F_c is the power of the anterior surface of the cornea, n the refractive index of the cornea and r the radius of curvature.

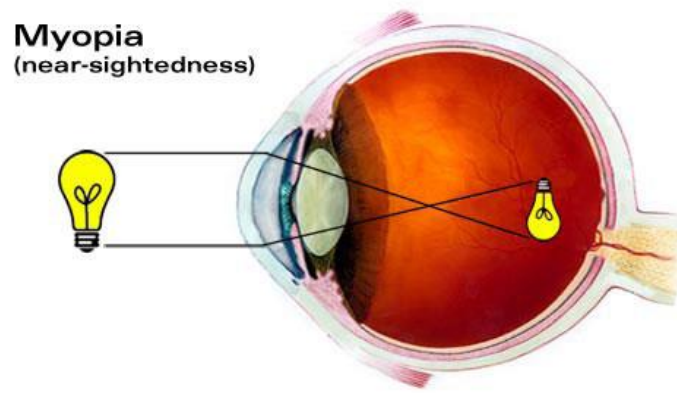


Fig.3 Myopic refractive error

1.2.4 Hyperopia

The hyperopic refractive error occurs when the far point is fantastic and located at a distance behind the cornea, and the incident beam of rays is focused behind the retina. (fig.4)

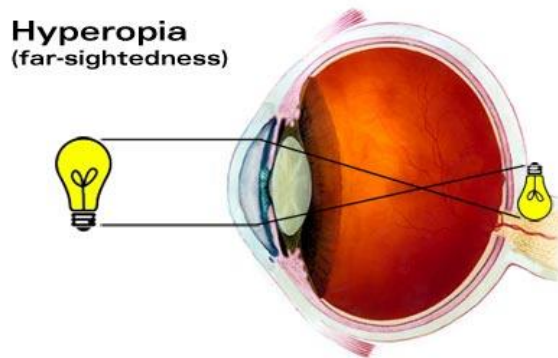


Fig.4 Hyperopia

1.2.5 Astigmatism

In astigmatism, the incident beam of rays is not refracted the same in all meridians so the eye does not have the same refractive power in all meridians. As a result, the radii are not focused at a point and we see two focal lines, usually perpendicular to each other, which form the conoid of Sturm.(fig.4.2)

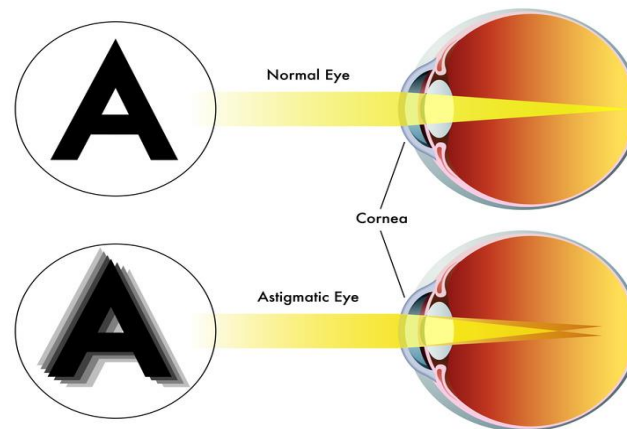


Fig.4.2 Astigmatism

1.3 Age and refractive errors

It is known that the eyes of each newborn human suffering from hyperopic refractive error. This error is eliminated in the next few years of life through the process of emmetropization, where the perfect match is achieved between the axial length of the eye and the total refractive power. The mechanism of emmetropization, utilizing optical signals, adjust the axial length of the eye, so that the focal plane (measured from the surface of the cornea), lie on the retina and remain there, due to achieve maximum sharpness of the image.

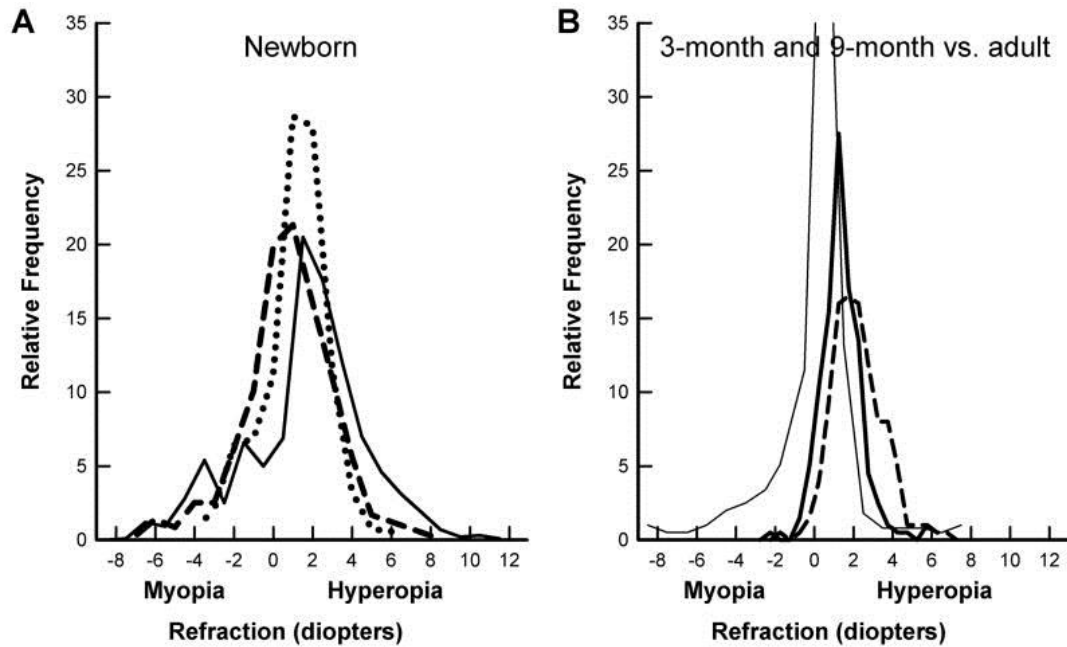


Fig.5 Refractive error distribution at birth from three studies; dashed line, Cook & Glasscock, solid line: Goldschmidt and dotted line, Zonis & Miller. B. Refractive distribution at 3 months (dashed line) and 9 months of age (dark solid line) from Mutti et al.¹⁰ compared with an adult distribution (thin solid line). At birth, the refractive distribution is broad. This narrows rapidly so that by nine months, nearly all children are emmetropic or slightly hyperopic. In adults, the distribution is narrower, but myopia has become more prevalent.¹

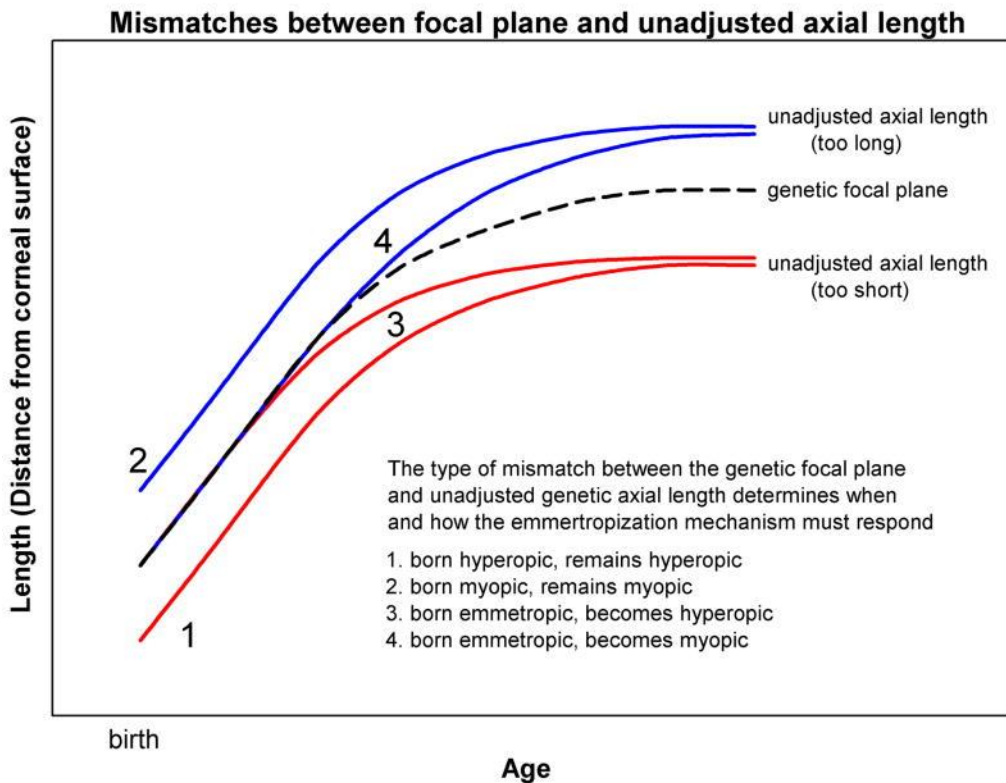


Fig.6 Hypothetical postnatal growth of the focal plane modeled as the log of age (dashed line) and four of the many possible growth patterns for the genetically-guided, unadjusted axial length. “1” and “2” depict unadjusted axial growth that is parallel to the focal plane, but either shorter or longer starting at birth so that, without an emmetropization mechanism, the eyes would remain either hyperopic (“1”) or myopic (“2”). “3” and “4” depict unadjusted axial growth that initially is the same as the focal plane, but diverges later in the postnatal period, creating eyes that would become either hyperopic (“3”) or myopic (“4”).¹

On a hyperopic eye, the retina is situated in front of the focal plane. The retina detects hyperopia and creates an increase in the rate of axial elongation of the growing eye by altering the biochemical and biomechanical properties of sclera. Thus, the moving of the retina to the focal plane is achieved, in order to the neutralization of hyperopia.

1.3.1 Emmetropization

The age (early school years) in which the emmetropization takes place, is the most critical for the development or not of myopia. For ages 45-50 years, we have a turn to the hyperopic errors due to eye accommodation failure (onset presbyopia), while even older (over 70 years) there is a tendency to myopic refractive errors due to biochemical changes in the structure of the crystalline lens.

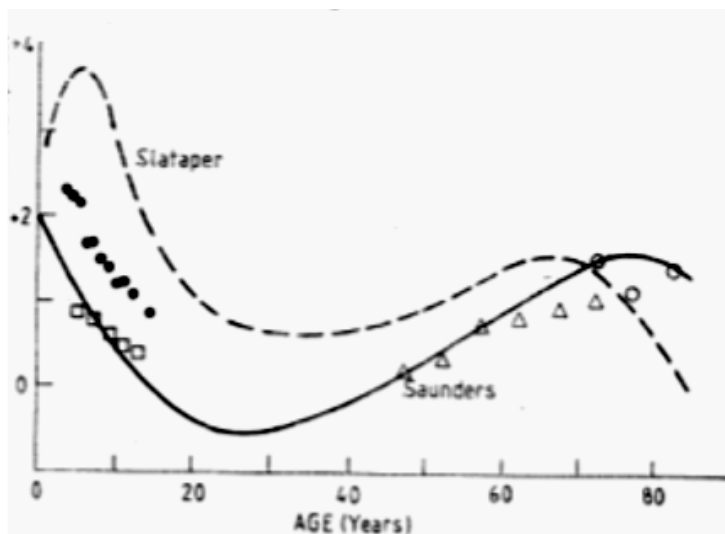


Fig.7 Development of refractive error with age

It is generally accepted by the scientific community that the age-related change in myopic error in schoolchildren, is caused by the axial elongation of the eye. After the first two years of life, the strength of the cornea remains constant while the axial length continues to increase, resulting in a myopic change of refraction during ocular growing. At this stage there is a change in the distribution of refractive error, from the normal distribution in a more compressed and sharp distribution. Such changes are the active processes that are intended to achieve emmetropia by matching, as mentioned above, the axial length of the eye to its total dioptric power.

The axial length is a major structural component of emmetropization. Due to the inability of the crystalline lens and the cornea to balance axial elongation occurring during emmetropization, causes myopia. The lens shows three times more compensatory changes in the refractive power, from those of cornea. The changes of both these structures the eye, follows the changes in axial length. A set of several studies connect the refractive error of the eye with the axial length, which makes clear the influence of axial length in the process of emmetropization. There is a kind of genetic determination of the axial length at birth, due to the interaction of a number of genes. The sclera is what determines the position of the retina and the axial length, during the development process. Therefore, such a growth process, determined by genetic factors that control the physiology of sclera, which are: cell division of fibroblasts, the quantity of produced collagen, the composition of its ingredients like glycosaminoglycans and cellular attachments. The axial length is a very important index of structural changes of myopia, and its measurement is possible because of some machines such as the Zeiss IOL Master.

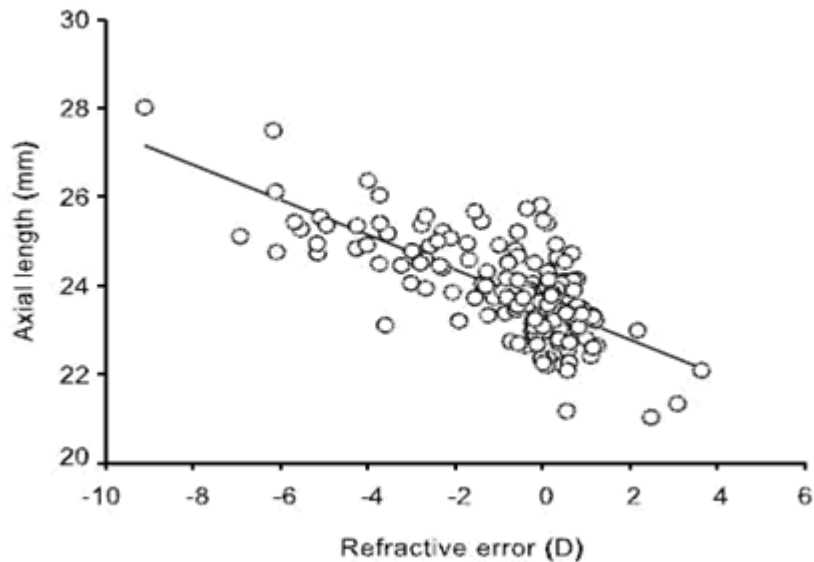


Fig.8 The graph shows the statistically significant dependence of the refractive state from the axial length ($P < 0,001$) in a university population aged 17-35 years. It becomes clear the myopic change by the increase of the axial length ($y = 0,4x + 23,59$). The average axial length was 23.88 mm, and was determined with IOL Master Zeiss. The average refractive error was -0,76 D, attributable to the characteristics of the studied population (age, education).²

1.4 Distribution of myopia in population

Global refractive errors have been estimated to affect 800 million to 2.3 billion.⁵ The incidence of myopia within sampled population often varies with age, country, sex, race, ethnicity, occupation, environment, and other factors.^{6,7} Variability in testing and data collection methods makes comparisons of prevalence and progression difficult.⁸

The prevalence of myopia has been reported as high as 70–90% in some Asian countries, 30–40% in Europe and the United States, and 10–20% in Africa.⁷ Myopia is about twice as common in Jews than in people of non-Jewish ethnicity.⁹ Myopia is less common in Africans [68] In Americans between the ages of 12 and 54, myopia has been found to affect African Americans less than Caucasians.¹⁰

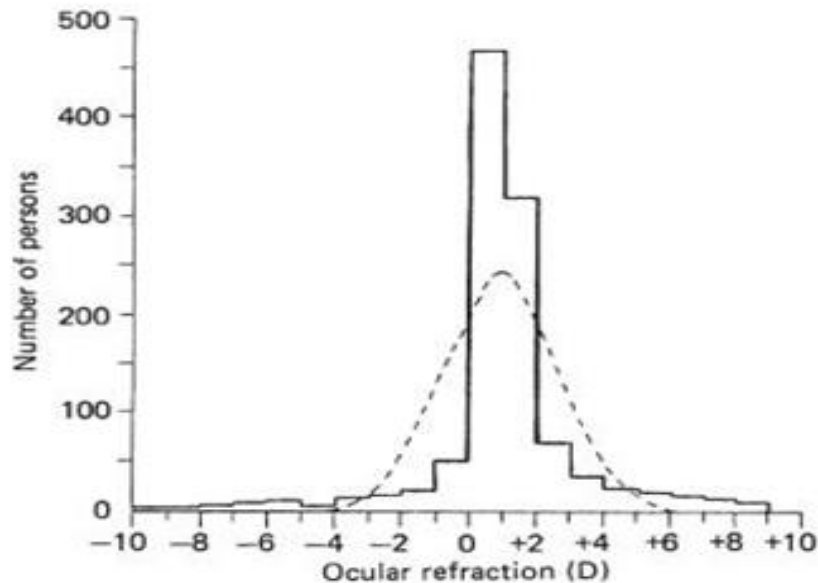


Fig.9 Typical example of the distribution of refractive error in an unselected population (based on 1033 young men, after Sorsby et al.) The dotted curve represents the corresponding normal distribution.³

1.4.1 ASIA

Myopia is very common in some parts of Asia.

In Singapore more than 80% of the population has myopia.¹¹

The myopic people in China are 400 million. That equals to the 31% of its population. The prevalence of myopia in high school in China is 77.3% and the myopia rate in college is more than 80%.

In Malaysia, up to 41% of the adult population is myopic to 1D and up to 80% to 0.5D.¹²

In Jordan, the myopic rate in adults aged 17 to 40, is 53.7%.¹³

In India though, only 6.9% of the population is myopic.^{14,15}

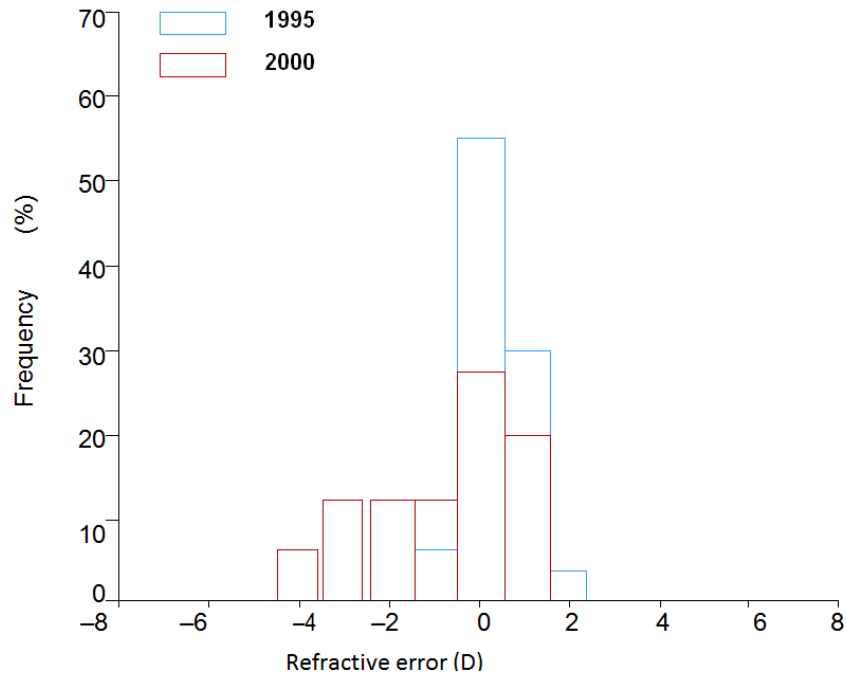


Fig.10 Changes in the refractive error distribution over a 5-year time interval for the same group of Hong Kong children with initial mean age 5 years (after Fan et al.).⁴

1.4.2 EUROPE

In the UK, the prevalence of myopia among first-year undergraduate students was found to be 50% of British whites and 53.4% of British Asians.¹⁶

In Greece, 36.8% of people aged 15 to 18 were found to be myopic.¹⁴

Western Europeans aged 40 or over have at least 1D of myopia, and 4.6% have at least 5D.¹⁷

1.4.3 NORTH AMERICA (UNITED STATES)

The prevalence of myopia in people aged 12 to 54 was 25% in 1971-1972, but in 1999-2004, myopia prevalence in the same aged population, was estimated to 41.6%.¹⁸

A study of 2,523 children aged 5-17 years found that the 9.2% have at least 0.75D of myopia. The highest prevalence was in Asians (18.5%) followed by Hispanics (13.2%). In African Americans the rate was 6.6%, and the lowest prevalence of myopia was in Caucasians (4.4%).¹⁹

A recent review found 25.4% of Americans aged 40 or over have at least -1.00 diopters of myopia and 4.5% have at least -5.00 diopters.¹⁷

1.4.4 AUSTRALIA

The 17% of Australia's population is myopic²⁰ and 8.4% of Australian children (aged 4-12 years) were found to have myopia greater than 0.5D.²¹ Australians aged 40 or over have at least 1D of myopia and 2.8% have at least 5D.¹⁷

1.4.5 SOUTH AMERICA (BRAZIL)

The prevalence of myopia in Brazilians aged 12 to 59 years, with 1D of myopia or more were found to be 6.4% due to a study in 2005.²² Another study found that in the city of Natal, 13.3% of the students were myopic.²³

Country	n	Age (years)	Prevalence of myopia	
			Criteria	%
UK	7600	7	< -1.00 D	1.1
Sweden	1045	12-13	≤ -0.50 D	45
USA	2583	6-14	≤ -0.75 D	10.1
USA	2523	5-17	≤ -0.75 D	9.2
African American	534			6.6
Asian	491			18.5
Hispanic	463			13.2
White	1035			4.4
Australia	2571	5	< -0.50 D	2.8
		12	< -0.50 D	8.7
Singapore	1453	7	≤ -0.50 D	29.0
		8	≤ -0.50 D	34.7
		9	≤ -0.50 D	53.1
Hong Kong		13-15		
Local school	335			85-88
International school	789			43 in non-Chinese 65 in mixed Chinese 80 in Chinese

Table 1. Geographic prevalence of myopia (a 2000 study).

The urban centers of East Asia (Hong Kong, Singapore) sometimes show epidemic rates, while evidence is less clear for the societies of Europe, Australia and the United States. It is worth noting that even within the population of the United States, individuals, primarily from Asia and Latin secondly, show the highest prevalence of myopic error. This fact is suggestive of a genetic predisposition of certain ethnic groups, which exert its effects irrespective of place of residence.²

2) KERATOCONUS

2.1 Definition²⁴

Keratoconus is a clinical term used to describe a condition in which the cornea assumes a conical shape because of thinning and protrusion(fig.11). The process is noninflammatory. Cellular infiltration and vascularization do not occur. It is usually bilateral, and although it involves the central two-thirds of the cornea, the apex of the cone is usually centered just below the visual axis. This disease process results in mild to marked impairment of visual function.

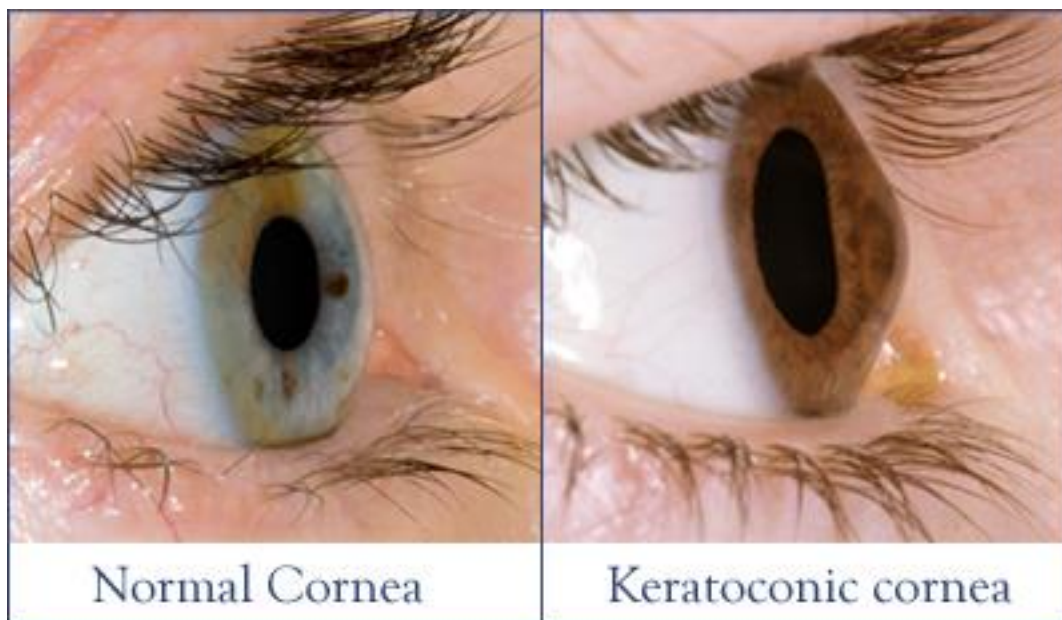


Fig.11 Normal Cornea vs Keratoconic cornea

2.2 Prevalence, distribution and course²⁴

Reported estimates of the prevalence of keratoconus vary widely, because of the variation in diagnostic criteria. Most estimates fall between 50 and 230 per 100000. Keratoconus occurs in people of all races. There is no significant gender predominance.

Keratoconus usually occurs bilaterally. In a large series done prior to the advent of computer-assisted topography the incidence of unilateral disease was found to be 14.3%. Although unilateral cases occur, it has been convincingly shown that when diagnostic criteria and computer-assisted topographical analysis allow the detection of very early keratoconus in the fellow eye the incidence is probably in the range of 2-4%.

The onset of keratoconus occurs at about the age of puberty. The cornea begins to thin and protrude, resulting in irregular astigmatism with a steep curvature. Typically, over a period of 10 to 20 years process continues until the progression gradually stops. If a faint, broad iron rings was present, it becomes a thinner, more discrete ring. The rate of progression is variable. The severity of the disorder at the time progression stops can range from very mild irregular astigmatism to severe thinning, protrusion, and scarring requiring keratoplasty.

2.3 Associated disease²⁴

2.3.1 Systemic disease

Over the past half-century much has been written linking keratoconus to atopic disease. The largest controlled study found a positive history of atopic disease in 35% of 182 keratoconus patients as compared to 12% of 100 normal control patients.

The thorough evaluation of the keratoconus patients should include a complete history of atopic disease. Appropriate referrals can be made if significant atopic disease is newly revealed. Allergic lid and conjunctival disease can affect contact lens tolerance adversely. As a result, surgical intervention may be required earlier in the course of the disease to affect visual rehabilitation.

Rados was the first to report association between Down's syndrome and keratoconus. Most series report the incidence as between 5.5% and 15%. Keratoconus also occurs with increased frequency among developmentally delayed individuals without Down's syndrome and the incidence of unilateral disease may be substantially higher in this group compared with general population.

Two plausible explanations for this association with keratoconus are that genetic abnormalities induce structural or biochemical changes resulting in the well-recognized phenotype or that eye rubbing causes the condition. Corneal hydrops occurs with increased frequency in patients with

Down's syndrome or other forms of intellectual impairment and this may also result from habitual ocular massage.

Keratoconus is associated with Ehlers-Danlos syndrome and osteogenesis imperfect. It has also been associated with some disorders of connective tissue, such as congenital hip dysplasia, oculodentodigital syndrome, Rieger's syndrome, anetoderma and focal dermal hypoplasia.

Seiler's theory is that diabetes offered a protective effect regarding keratoconus, based on a large case-controlled study. According to this study, the incidence of manifest diabetes was significantly lower in the keratoconus group, than the normal patients.

Keratoconus patients found to be less conforming and more passive-aggressive, paranoid and hypomanic than normal control individuals(Mannis et al) ,and in a small study(Swartz et al) was found that after penetrating keratoplasty, the incidence of abnormalities in psychological testing was less than before surgery.

2.3.2 Ocular disease

Retinitis pigmentosa seems to be associated with keratoconus, according to many authors. Infantile tapetoretinal degeneration is frequently complicated by keratoconus. Alstrom's and Olson's study shows that more than 35% of patients with this disease (older than 45 years old) had keratoconus.

Keratoconus has also been reported with retinopathy of prematurity, progressive cone dystrophy, aniridia, iridoschisis, and essential iris atrophy.

Finally, Totan and his associates found a relation between conical cornea and vernal conjunctivitis, by evaluating 82 vernal patients with videokeratography , and Tuft et al in a study of 37 patients with atopic keratoconjunctivitis found keratoconus to be an important cause of vision loss in that kind of patients.

2.4 What causes Keratoconus?

The exact cause of Keratoconus is unknown. There are many theories based on research and its association with other conditions. However, no one theory explains it all and it may be caused by a combination of things.

Genetics, the environment and endocrine system is believed that play a role in keratoconus.

2.4.1 Genetic Causes

One scientific view is that keratoconus is developmental (i.e., genetic) in origin because in some cases appear to be a familiar association. From the presently available information there is less than one in ten chances that a blood relative of a keratoconic patient will have keratoconus. The majority of patients with keratoconus do not have other family members with the disease. Some studies show that keratoconus corneas lack important anchoring fibrils that structurally stabilize the anterior cornea. This increased flexibility allows the cornea to “bulge forward” into a cone-shaped appearance.

2.4.2 Environmental Causes

Eye rubbing: Keratoconus is associated with excessive eye rubbing. Something that has not been proven but has been suggested as a possible cause of keratoconus is the poorly fit contact lenses that rub against the irregularity of the keratoconic cornea.

Allergies: The connection between keratoconus and allergic disease remains unclear, but many keratoconic patients report allergies which cause itching and irritation, leading to eye rubbing.

Oxidative stress: Keratoconic corneas lack the ability to eliminate the free radicals (harmful byproducts of cell metabolism) as normal corneas do. The free radicals stay in the tissue and can damage the collagen (the structural part of the cornea).

2.4.3 Hormonal causes

Another hypothesis is that the endocrine system may be involved because keratoconus is generally first detected at puberty and progresses during pregnancy. This theory is still controversial and has not been proven.

2.5 Keratoconus symptoms and signs^{25,26}

2.5.1 Symptoms

Keratoconic patients present for optometric assessment with blurred vision, usually in one eye. Symptoms like photophobia, eye-strain, monocular polyopia with multiple ghost images, flaring around light sources and a history of worsening and variable myopia and astigmatism are common. Spectacles and soft contact lenses are unable to correct the refractive error, and a correction with rigid contact lens is necessary.

2.5.2 Signs

Early signs:

- Irregular oblique astigmatisms if often revealed by refraction
- Ophthalmoscopy or retinoscopy shows an irregular 'scissor' reflex
- Keratometry shows high irregular astigmatism (axis that do not add to 180 degrees)
- Rizutti's sign or a conical reflection on nasal cornea when a penlight is shone from the temporal side
- Slit-lamp shows Vogt lines (vertical deep stromal striae), which generally disappear with firm pressure applied over the globe, and re-appear when pressure is discontinued (fig.12)
- Fleischer ring, an iron (hemosiderin) deposit often present within the epithelium around the base of the cone. It is yellow-brown to olive-green in color and best visualized with a cobalt blue filter
- The nerves of the cornea may be more visible
- Inferior corneal steepening, identified by corneal topography

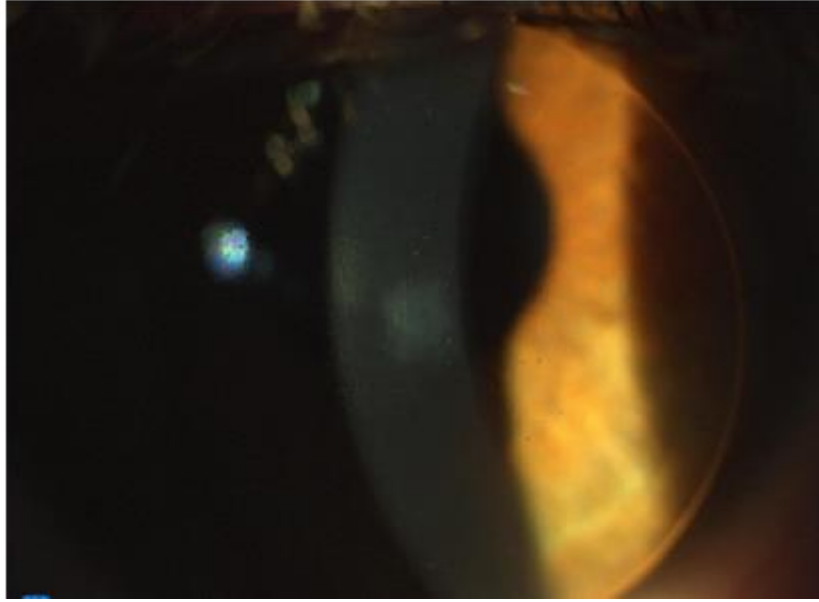


Fig.12 Vogt's Striae sign. Vertical lines in Descemet's membrane are noted.

Late signs

- Munson's sign, a protrusion of the lower eyelid in down gaze(fig.13)
- Superficial scarring
- Break's in Bowman's membrane
- Acute hydrops, a condition where a break in Descemet's membrane allows aqueous into the stroma causing severe corneal thickening, decreased vision and pain
- Stromal scarring after resolution of acute hydrops, which paradoxically may improve vision in some cases by changing corneal curvature and reducing the irregular astigmatism.

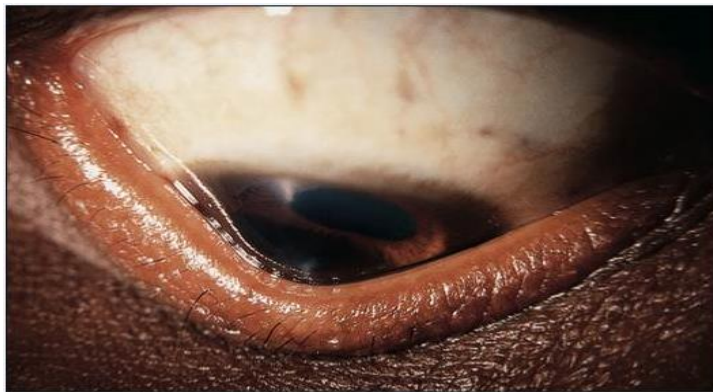


Fig.13 Corneal protrusion causing bulging of the lower lid on down gaze (Munson sign).

2.6 Classification ²⁴

- Keratometry: mild (<45D); advanced (up to 52D); or severe (>52D)
- Morphology: nipple (small: 5mm and near-central); oval (larger, below-center and often sagging); globus (more than 75 per cent of cornea affected)
- The corneal thickness: mild (>506µm); advanced (<446µm).

2.7 Diagnostic procedures ^{24,25}

The procedures include:

- Ophthalmic history of the patient, including the ocular history of the family, history of allergies, heritable disease etc.
- Slit-lamp examination
- Hard or gas permeable contact lens trial because good vision with lenses eliminates other sources of poor vision, including amblyopia
- K values measurements
- Ultrasound pachymetry
- Corneal topography(fig.14)

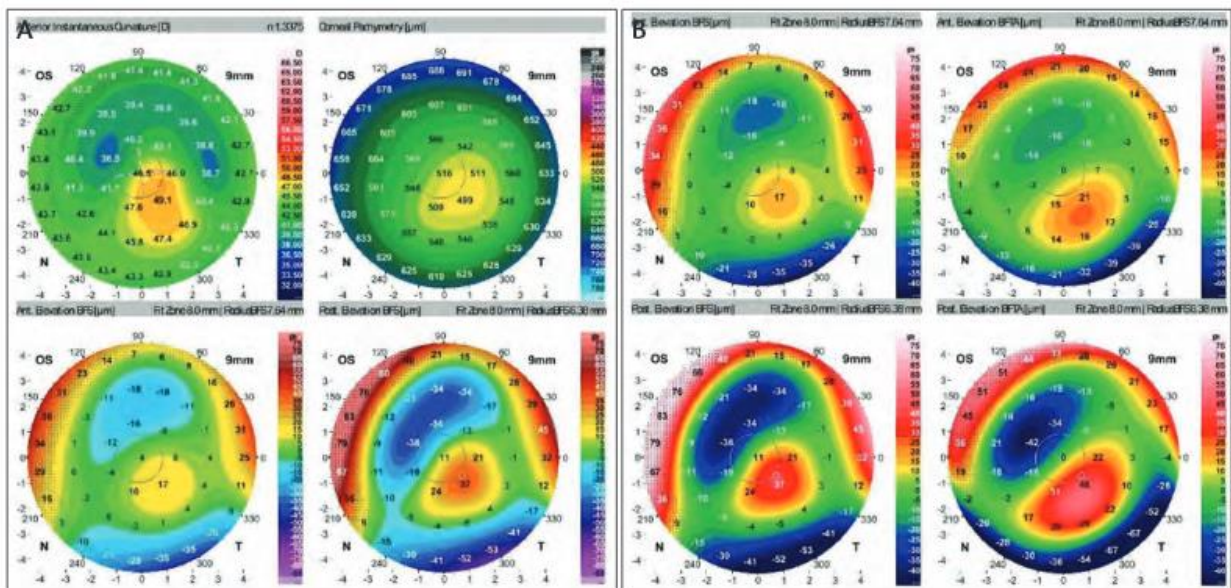


Fig.14 Dual scheinplflug system images that show the clear keratoconus throughout the left eye

2.8 Optical performance and keratoconus (influence)²⁷

The keratoconic cone dimension, location and surface influence the optical performance of the eye.

The location of the cone affects the spherical equivalent. Patients with central cones are more myopic and those with more peripheral cones less so. Spherical equivalent tends to be slightly hyperopic for an outlying cone.

Both the cone shape and location affect the cylindrical error.

Cone shape dominates when near the visual center, and far away from it, the location of the cone plays the major role on astigmatism's amplitude.

The less powerful meridian is the one that pointing to the cone apex. For an outlying cone, the spherical equivalent could be hyperopic, although the power in the perpendicular meridian is always myopic. An –against the rule- astigmatism exist, for an inferior cone at a 4 to 8 o'clock position.

The dimension of the cone affects strongly the high-order aberrations. Thus, when the cone dimension or cone location is comparable to the pupil size, the greatest, most visually significant high-order aberrations occur.

2.9 Management and treatment of keratoconus^{24,25,28}

In the mildest form of keratoconus, eyeglasses or soft contact lenses may help. But as the disease progresses and the cornea thins and becomes increasingly more irregular in shape, glasses and regular soft contact lens designs no longer provide adequate vision correction.

Treatments for moderate and advanced keratoconus include:

- a) Spectacles
- b) Custom soft contact lenses
- c) Gas permeable contact lenses
- d) "Piggybacking" contact lenses
- e) Hybrid contact lenses
- f) Scleral and semi-scleral lenses
- g) Penetrating keratoplasty (PTK)
- h) Deep Lamellar keratoplasty(DLK)
- i) Radial keratotomy
- j) Photorefractive keratectomy (PRK)
- k) Intra corneal rings segments
- l) Corneal crosslinking
- m) Topography-guided conductive keratoplasty

- a. Spectacles: spectacles are unable to correct the development of irregular astigmatism occurs in progressed keratoconus, thus they are used only in early cases of keratoconus
- b. Custom soft contact lenses: this type of lens is specially designed to correct mild-to-moderate keratoconus. These lenses are made to order for each and every keratoconic patient, based on detailed measurements of the person's keratoconic eye(s)
- c. Gas permeable contact lenses: Their rigid lens material enables gas permeable lenses to vault over the cornea, replacing its irregular shape with a smooth, uniform refracting surface to improve vision. But gas permeable contact lenses can be less comfortable to wear than soft contacts.(fig.15)

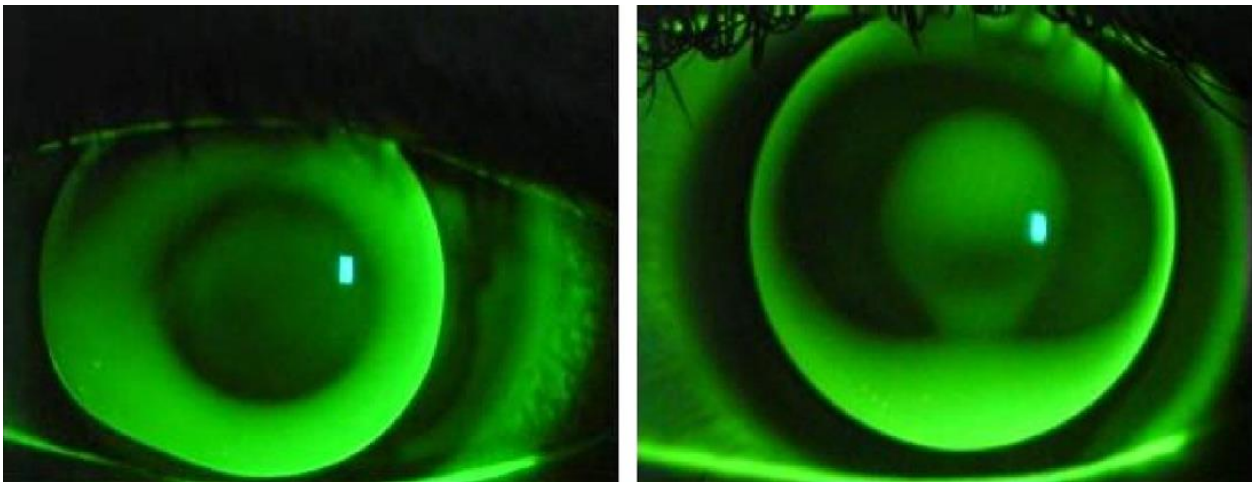


Fig.15 Fluorescein patterns of two different gas permeable contact lens fittings in keratoconus. The figure on the left shows a flat fitting with a significant touch of the lens on the central cornea. The figure on the right shows a three-point-touch fitting with slight central touch and peripheral bearing on the cornea.

d. "Piggybacking" contact lenses: a gas permeable contact lens is fitting on top of a soft contact lens. This approach increases wearer comfort because the soft lens acts like a cushioning pad under the rigid gas permeable lens.(fig.16)



Fig.16 Piggy-Back fitting in keratoconus.

e. Hybrid contact lenses: a combination of a highly oxygen-permeable rigid center with a soft peripheral "skirt."

f. Scleral and semi-scleral lenses: These are large-diameter gas permeable contacts — large enough that the periphery and edge of the lens rest on the sclera (white of the eye), they don't apply pressure to the cone and they are more stable than gas permeable lenses.

g. Penetrating keratoplasty (PTK): a surgical procedure in which the entire thickness of the cornea is removed and replaced by transparent corneal tissue. (fig.17)

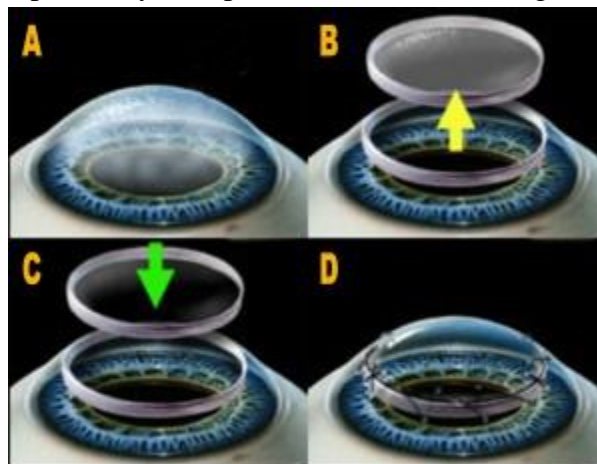


Fig.17 Penetrating keratoplasty procedure

h. Deep Lamellar keratoplasty (DLK): in this procedure superficial corneal layers are removed (Descemet's layer and endothelium remain intact) and replaced with healthy donor tissue.

i. Radial keratotomy: a technique in which longitudinal incisions along the peripheral cornea are performed. (no longer performed)

j. Photorefractive keratectomy (PRK): an excimer laser is used to ablate a small amount of tissue from the corneal stroma, in order to change permanently the shape of the anterior central cornea.

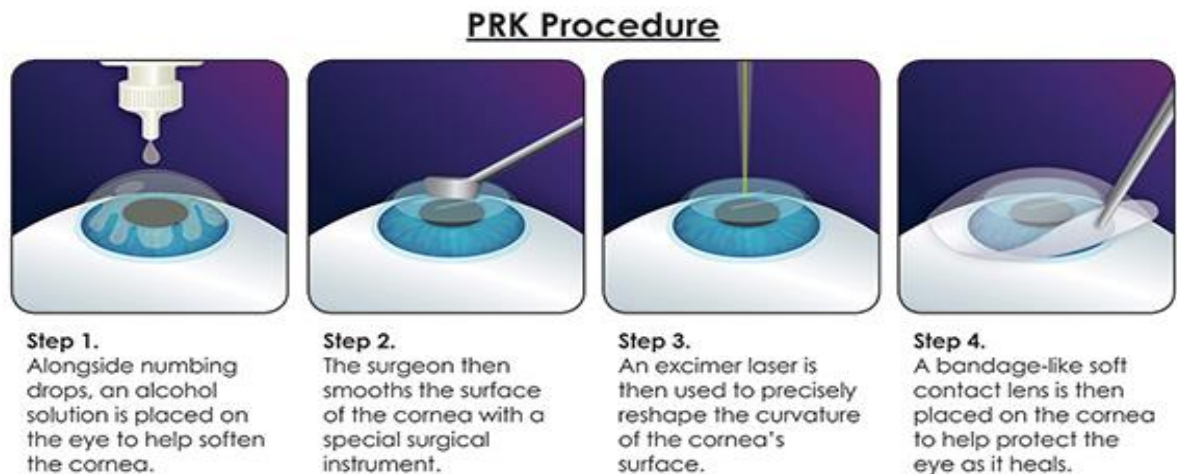


Fig.18 PRK procedure

k. Intra corneal rings segments: a technique in which one or two polymethyl methacrylate segments are implanted in the corneal stroma in order to reshape its abnormal shape.

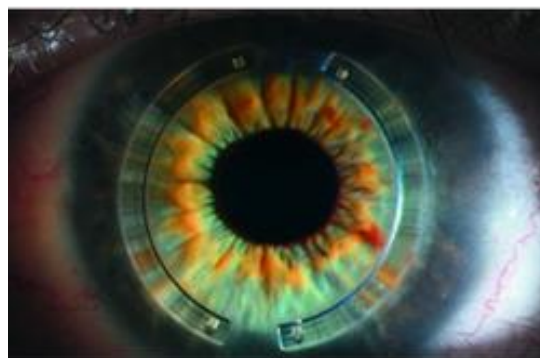


Fig.19 Intra corneal rings segments

l. Corneal crosslinking: a technique which aims to increase corneal rigidity and biomechanical stability by applying riboflavin and radiate the cornea with ultraviolet radiation in order to activate riboflavin and induce covalent bonds between collagen fibrils in the corneal stroma. This procedure, initially, involves removing the corneal epithelium in a 6-7mm diameter central zone(fig.20)

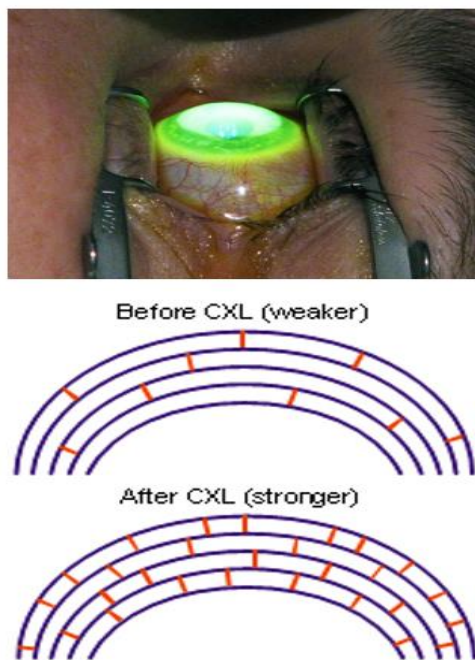


Fig.20 Corneal crosslinking –weak bonds between collagen fibrils, and strong bonds after the procedure

m. Topography-guided conductive keratoplasty: this treatment uses energy from radio waves, applied with a small probe at several points in the periphery of the cornea to reshape the eye's front surface. A topographic "map" created by computer imaging of the eye's surface helps create individualized treatment plans.

2.10 Aim of the study

The research aims, through a cross-sectional study in patients with keratoconus, to check whether the balance between axial length-corneal power is disrupted, and show us if a keratoconic eye is relatively "large" or not, which could assess the development risk factor of keratoconus. Also, by evaluating the binocular differences in a group of children / young people, who usually have keratoconus in different stages in both eyes, it will be checked whether these certain differences are connected with any difference in axial length and refractive error.

PART 2

3) METHODS

This study involves data from patients who come to the Vardinoyiannion Eye Institute of Crete (VEIC) and the University Hospital of Heraklion to get examined for keratoconus or for re-examination, and data collected by another side from Jos Rosema, University of Antwerpen, Belgium, since this is a collaborative project.

Both eyes' data will be recorded. These data are as follows:

- A) the refraction of the eye (by a refractometer and objective refraction)
- B) the axial length and the anterior chamber depth of the eye (by the IOL Master biometric system) .
- C) the curvature of the cornea(corneal topography by Galilei)

3.1 Subjective refraction

Subjective refraction is made by the following procedure.

Initially, there is a monocular evaluation of the vision without correction for each eye. Then, correction is placed on the phoropter(fig.21) according to the measurements of the Canon RK-F1 for the right eye, followed by clouding with the method of the fog. Throughout the process the other eye is covered. Then with refractive step of 0,25D the sphere and the cylinder are fluctuated until the best visual acuity. After, the crosscyl is used for final testing of astigmatism, and finally the subject is undergone to dichroic control. After having recorded the best visual acuity for the right eye, the same procedure for the left eye is followed.



Fig.21 Phoropter

3.2 Refractometer

3.2.1 Automatic refractometers²⁹

Automatic refractometers are consisting of:

1) A source of infrared light (800-900 nm)

the infrared radiation is used mainly due to the high transmittance and reflectance obtained from the deeper layers of the eye (sclera and choroid).

At this wavelength, the reflection from the sclera and choroid, in combination with the effect of extensive aberration, result an error of -0, 50 D which must be added to compensate the refraction for the natural light.

2) A fixation point

Several targets as "stars" or images with blurring in the periphery have been used, to achieve a relaxation of adaptation. Nowadays all automatic refractometers use clouding techniques for easing the adaptation before the objective measurement where usually a positive lens placed in front of the image to make the image blurry. However, the relaxation of the adaptation is not always achieved and there may be fluctuations up 0, 50 D resulting a small overcorrection in myopia or undercorrection in hyperopia or more in case of young people or children.

3) A Badal optometer

The Badal optometer used by most refractometers because it has two major advantages:

- There is a linear relationship between the distance of Badal lens from the eye and the refraction at the axis that we count.
- In this lens system, the magnification of the target remains fixed, despite the position of the Badal lens.

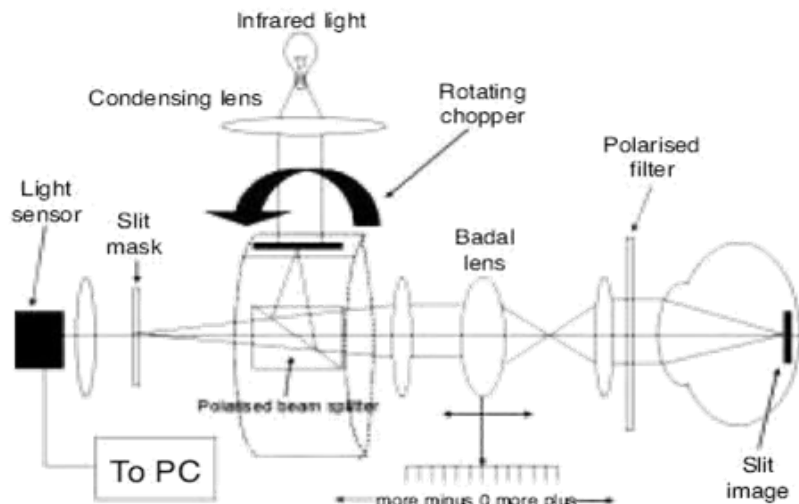


Fig.22 Basic principle of automatic refractometry

3.2.2 Canon RK_F1 automatic refractometer³⁰

The refractive error was also measured by the refractometer Canon RK-F1. This refractometer is a closed field refractometer and is widely used by optometrists because it is very easy to use and provides fast and reliable measurements.



Fig.23 Canon RK-F1

The patient sits and positioning the chin and forehead on the corresponding braces and is requested to look at the image in the refractometer, in this case a house. When the pupil of the subject is displayed the examiner presses the start button and the refractometer automatically makes aligning and measuring first on the right and then on the left eye. The procedure is fully automated.

The vertex distance is set to 12mm. The machine takes three measurements for each eye and uses their mean value.

3.3 IOL MASTER ZEISS

IOL master is a commercial tool for biometry, it defines the axial length of the eye using the technique of partial coherence interferometry (PCI), and measures the depth of the anterior chamber using optical pachymetry, taking at the same time keratometric measurements. (fig.24)



Fig.24 IOL master Zeiss

3.3.1 Axial length measurements^{31,32,34,35}

The determination of the axial length of the eye is a very important chapter in ophthalmological practices, since it is related to studies of refractive errors (e.g. myopia) (Wong et al., 2001), the cataract surgery and intraocular lens implantations (Haigis et al. 2000), as well as other pathologies of the eye (Cekic et al., 1999). The Zeiss IOL Master can measure the axial length of the eye with precision of about ± 0.01 mm (measuring range 14-39 mm) using partial coherence interferometry method, which is based on the Michelson interferometer.

This invention of the American physicist A. Michelson (1852 - 1931), uses a beam of light which through a partially reflective mirror (beam splitter) is firstly divided in two. Each part follows its own path, until at some point the two parts of the initial beam are recombined to produce thereby interference images and detected by an appropriate device (detector).

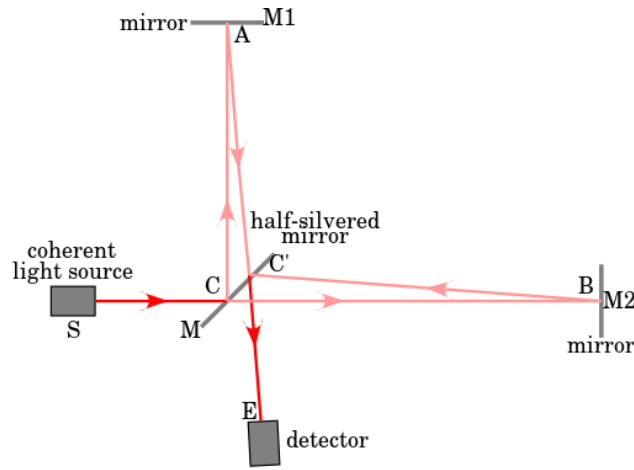


Fig25. A schematic representation of the main elements of the Michelson interferometer

If the distance between the movable mirror M1 and the beam splitter become greater or less by d than the corresponding distance of the fixed mirror M2 from the splitter, then it can easily be shown the relationship $d = m * \lambda / 2$ where λ the wavelength of the radiation of the beam and m is the number of the interference fringes that penetrate the detector ($m = 0, 1, 2 \dots$). According to this relationship it is possible to calculate very precisely unknown wavelengths or distances. Let's see how all this apply to the measuring mechanism of the axial length of the eye by the IOL Master.

Firstly, the diode laser (LD) device generates infrared light ($\lambda = 780\text{nm}$) and short length of coherence ($160\mu\text{m}$, approximately coincides to the axial resolution of the system). This means that the interference will be achieved only if the delays along the path of the interferometer harmonized within the coherence period of the light source. The above property makes the partial coherence interferometry the most appropriate method for describing gradient or uneven surfaces. Having therefore divided into two coaxial beams CB1 and CB2 by the beam splitter BS1, the light is reflected into the eye by the mirrors M1 and M2. The distance which separates the two beams will be equal to twice the displacement of the mirror M1 (d). Both coaxial rays entering the eye, which results in a reflection of both the surface of the cornea (C), and in melachroun epithelium of the retina (R). The difference of frequencies between coaxial rays exiting the eye (after passing a second beam splitter BS2) is detected by the photodetector (PHD). During the measurement, the mirror M1 moves at a constant speed, causing a change in frequency of the reflected coaxial light which is detected by the photodetector because of Doppler phenomenon. The displacement d of the mirror M1 can be determined very accurately and be related to the reflected signals detected at the photodetector, thus allowing accurate measurements of the axial length (AL) of the eye.

For the determination of the axial length of the eye, taking five valid measurements required (Signal to Noise Ratio - SNR > 2.0) of which the average is calculated, if they do not differ more

than 0.1 mm. Otherwise, divergent measurements should be repeated, to calculate the axial length accurately. Finally, it is worth mentioning that Zeiss constitutes a) take not more than 20 measurements of axial length in each eye every day for safety reasons, and b) avoid measurements in eyes that have undergone retinal detachment.

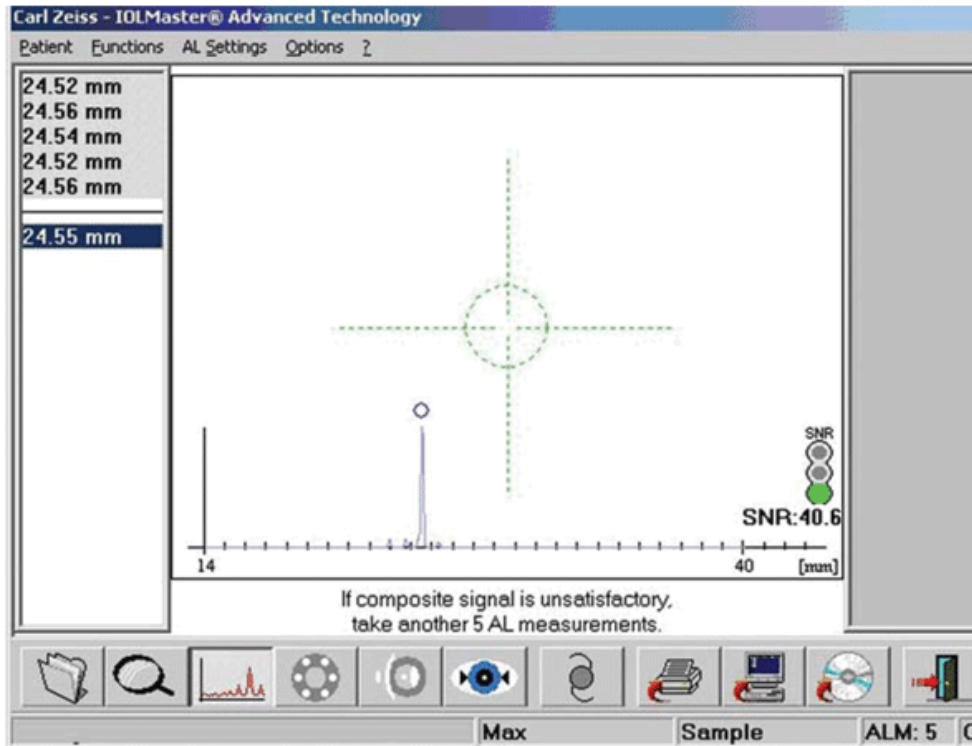


Fig.26 Axial length (shown here after five single measurements) is now calculated via digital signal processing instead of simply averaging acceptable-quality measurements. This dramatically improves signal-to-noise ratio (lower right on screen). The green "traffic light" signal indicates that conditions are ideal for continued measurements.

3.3.2 Measurement of anterior chamber depth (ACD) ^{31,33}

The depth of the anterior chamber defined as the distance measured parallel to the optical axis, from the epithelium of the cornea until the anterior surface of the crystalline lens. The determination of the depth of the eye's anterior chamber can give important information in various fields of ophthalmology. In support of this view, we could say that such a measure: a) contributes to increasing the accuracy of determining the power of the intraocular lens in a cataract surgery, b) is a fairly reliable glaucoma indicator, as glaucomatous patients tend to have more shallow anterior chamber (Devereux et al., 2000), and c) assist in the proper evaluation of the diameter of the part of the optic zone which excised during a photorefractive keratectomy using excimer laser.

The IOL Master of Zeiss is able to measure the depth of the anterior chamber of the eye with precision ± 0.01 mm and with a measuring range of 1.5 - 6.5 mm. To achieve this, it projects a slit beam of width 0.7 mm onto the anterior segment of the eye to the corner of 38° with the visual axis. Then, the CCD camera of the device takes multiple images of the eye part that is illuminated through the front chamber and by this method the distance between the posterior part of the cornea and the anterior surface of the crystalline lens is defined. This means that, to determine the depth of the anterior chamber, we must subtract the corneal thickness, from the distance measured above. Thus, if prior to measuring the depth of the anterior chamber has executed a valid keratometric measurement the IOL Master, the software automatically uses the calculated radius, to determine the depth accurately. If for any reason the device was not able to calculate the radius of curvature of the cornea, the IOL Master will ask the user to enter it manually. If the cornea is astigmatic, the IOL Master will ask to register the values of the radius of each of the two principal meridians, to make the final calculation of the depth of the anterior chamber.

Aligning –and the measurement procedure especially for pupils of a short diameter- requires experience and practice on the part of the examiner and cooperation on the part of the person who get tested. The examiner, after asking from the subject to adherence to the yellow light – target, aligns the device so that the focal point is between the images of the cornea and eye lens or else be very close to the optical part of the lens(fig.27) . After all that happened, by pressing the button on the joystick, device automatically takes five measurements of the depth of the anterior chamber from which the average value is calculated. If any of the measurements differs from the other more than 0.1 mm, then the average value is not calculated and the test should be repeated for security reasons. The IOL Master is not able to measure the depth of the anterior chamber in pseudophakic eyes. Any results arising from such an arbitrary measure would be totally wrong. Finally, the measurements obtained by the IOL Master for the depth of the anterior chamber may be problematic in cases of bad focusing of the device (defocus) or incorrect alignment, eyes with glaucoma, dry eyes and defects of the cornea.

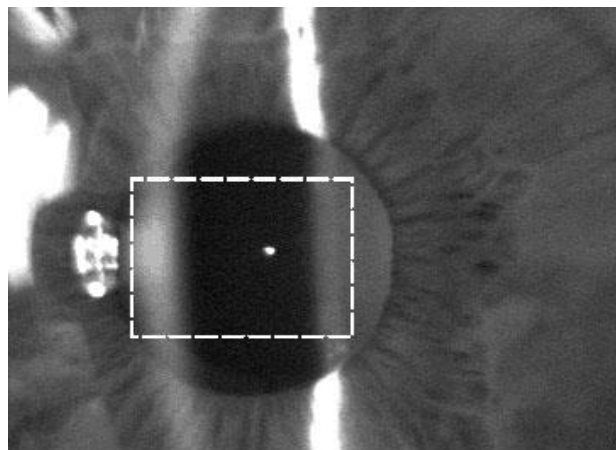


Fig.27 Alignment for anterior chamber depth measurement

3.3.3 Keratometry³¹

Keratometry is known as an objective method by which we can measure the radii of curvature and thus the refractive power of the cornea in different meridians. Thus, the corneal astigmatism of the central area with a diameter of about 3 mm can be calculated.

For the measurement of the radii of curvature of the cornea, the IOL Master projects on the cornea, using infrared light diodes, six light points which are arranged in a hexagonal design with a diameter of about 2.3 mm.(fig.28) The light of these points, at first is reflected in the tear film of the cornea, and then returns back into the machine where it is shown by a CCD camera. Then, the software of the IOL Master measures the distance between the reflections of the opposite points of the light for the three pairs and thereby identify: a) the radii of curvature of the cornea b) the refraction of the cornea and c) the astigmatic difference, of the three defined meridians.

IOL Master's scale for measuring the radius of curvature of the cornea is 5 - 10 mm, while the accuracy according to Zeiss reaches ± 0.01 mm. It should be noted that the calculation of refraction is based on both the measurement of the radii of curvature of the cornea and its refractive index. The IOL Master uses as a corneal refractive index the value 1.332 (default). This results slightly different results in comparison with other manufacturers. To make the results comparable to other keratometric devices, IOL Master allows the selection of the refractive index.

The measurement process is relatively simple. The person who get tested, focuses on a specific target (yellow light), while the examiner brings the device so that the six peripheral points are symmetrical in a circular crosshair and appear well focused. Once the subject is blinking to avoid eye dryness, three measurements are taken separately (length measuring 0.5 sec) and their mean values will be calculated. If measurement results differ more than 0.05 mm (quite rare), the mean value cannot be calculated and the test is repeated for security reasons.



Fig.28 Focus of the six points of light in a regular hexagonal order

The main reasons that the measurements can differ considerably include poor focus of the device (defocus), the blink of the person who get tested during the measurement, the eye with intraocular lens, dry eye and abnormalities on the surface of the cornea (scarring).

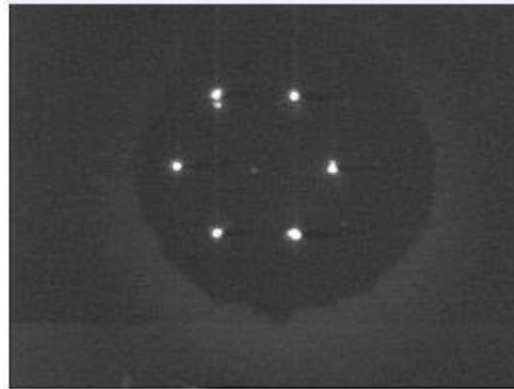


Fig.29 Multiple reflections produced by a dry eye

3.4 The GALILEI™ Dual Scheimpflug Analyzer^{36,37}

The GALILEI™ Dual Scheimpflug Analyzer (Ziemer Group; Port, Switzerland) is a device for corneal and anterior segment analysis that combines Placido-based corneal topography and dual Scheimpflug anterior segment imaging. The integrated system exploits the advantages of both technologies in a single exam, along a common reference axis.

3.4.1 Dual Scheimpflug Imaging

The principal advantage of Dual Scheimpflug imaging is that corresponding corneal thickness data from each view can simply be averaged to compensate for unintentional misalignment, which results in a corrected measurement value at the corresponding location. The dual Scheimpflug imaging principle is independent of inclined surfaces, and thus allows accurate pachymetry without knowledge of the actual decentration of the slit from the apex. In Figure 30, the dual Scheimpflug principle is graphically illustrated. Figure 31 shows the result of a theoretical calculation of simulated deviations from the true thickness values, as seen from both

Scheimpflug views, for all off centered cases up to ± 1 mm with respect to the corneal apex. The deviation is as high as $30 \mu\text{m}$ at 1 mm decentration or approximately $10 \mu\text{m}$ in the case of 0.3 mm decentration, well within the range of motion of a normal eye during target fixation. Simple averaging of the thicknesses in the two corresponding Scheimpflug views reduces this error by a factor of 10, without the need for correcting the misalignment.

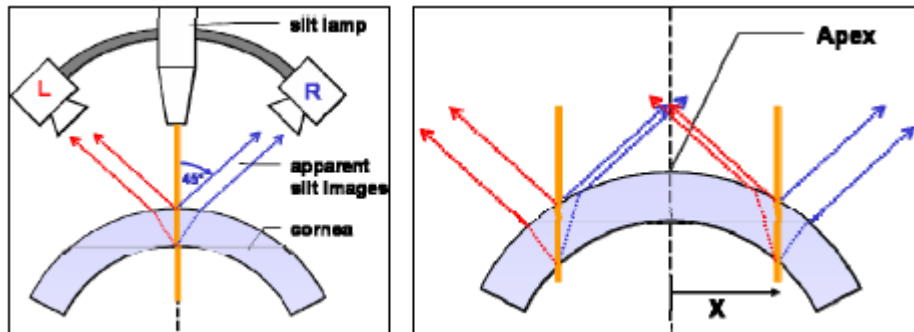


Fig.30a In the centered instrument condition, the apparent slit images in both Scheimpflug views are identical. The slit light is perpendicular to the spherical surface; therefore the viewing angles for both cameras are equal.

Fig.30b In the decentered condition, either left or right, the apparent slit images are no longer identical. The slit light is not perpendicular to the surface. Therefore, the apparent slit image is thicker in the left view and thinner in the right view, or vice versa, depending on the direction of decentration.

The principle of averaging two measurement values of the same object, which are related in a reciprocal manner, is a well-known method. The two Scheimpflug channels in the GALILEI™ device are optically identical; they are opposite to each other and aligned symmetrically to the rotational axis which contains the slit light. When the slit light is rotationally scanned while centered on the corneal apex, the apparent thicknesses of both views are identical, as illustrated in

Figure 30a. If the slit light is not centered on the corneal apex, the optical condition can be regarded as inclined to the surface. Living human eyes are always in motion even under perfect fixating conditions, and scanning takes time. Therefore, the rotational device axis may become decentered from the aligned apex position during the course of the rotational scan acquisition. In

this situation, the projected slits impinge upon the anterior surface of the cornea inclined, resulting in two apparent slit images deviated from each other in thickness, as seen in Figure 30b. The reciprocal relationship of the dual views allows simple averaging of the corresponding thickness values to correct the values at each of the slit positions, as demonstrated in Figure 31. The dual Scheimpflug system has only to take into account decentration and allocate each averaged thickness and posterior height value to its proper location, whereas single Scheimpflug systems additionally have to make estimations on the variable surface inclination for calculating correct thicknesses or posterior heights.

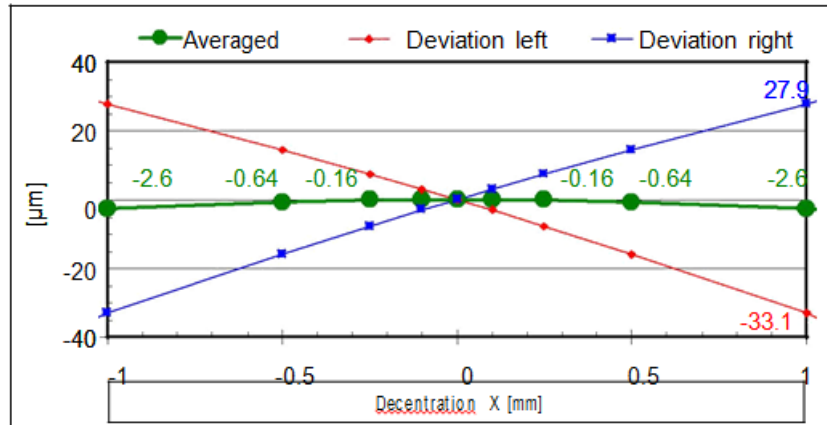


Fig.31 This graphic simulates the apparent thickness deviation of a spherical cornea with a thickness of 500 μm and a decentration of up to ± 1 mm. The thickness deviations from the true value are represented in red and blue, as seen from the left view and from the right view, respectively. Simple averaging of the corresponding thickness values reduces the deviation by a factor of ten without need of correcting for decentration.

3.4.2 Rotational Scanning

The GALILEI™ Dual Scheimpflug Analyzer is a rotational system, acquiring a user-defined number of images as the camera rotates around the central axis. A rotational scan is stable, readily achieved by a single motor driven axis, and takes into account the natural symmetry of the human eye. Images are segmented, and the extracted surfaces of the anterior segment of the eye may be displayed independently or reconstructed in three dimensions. A scanning system takes time to acquire the necessary images, and therefore eye motion must be corrected for proper surface representation. Generally, the longer the scan acquisition time, the larger is the eye movement that must be tracked and incorporated into the calculations. In the GALILEI™ System, both Placido and Scheimpflug data are acquired simultaneously as the camera rotates, and then a motion correction algorithm applied to the combined dataset. An appropriate 3D analysis of the anterior chamber also allows planning for placement of phakic IOLs, as well as lens densitometry applications.

3.4.3 The GALILEI™ Software Interface

The software interface allows the user to view the acquired Placido or Top View image and simultaneously acquired Scheimpflug images, either left or right, as illustrated in Figure 32. The schematic eye diagram in the upper left corner shows the orientation of the slit as it rotates over the eye. The Scheimpflug view displayed can be determined by the color of the dot in the corner

of the image, on the schematic eye, and on the toggle switch below the schematic eye. In Figure 32a, the dot is orange and the slit is aligned horizontally, both of which correspond to the view from the camera in the superior position on the schematic eye. To view the image acquired from the inferior position, the toggle with a blue dot would be chosen.

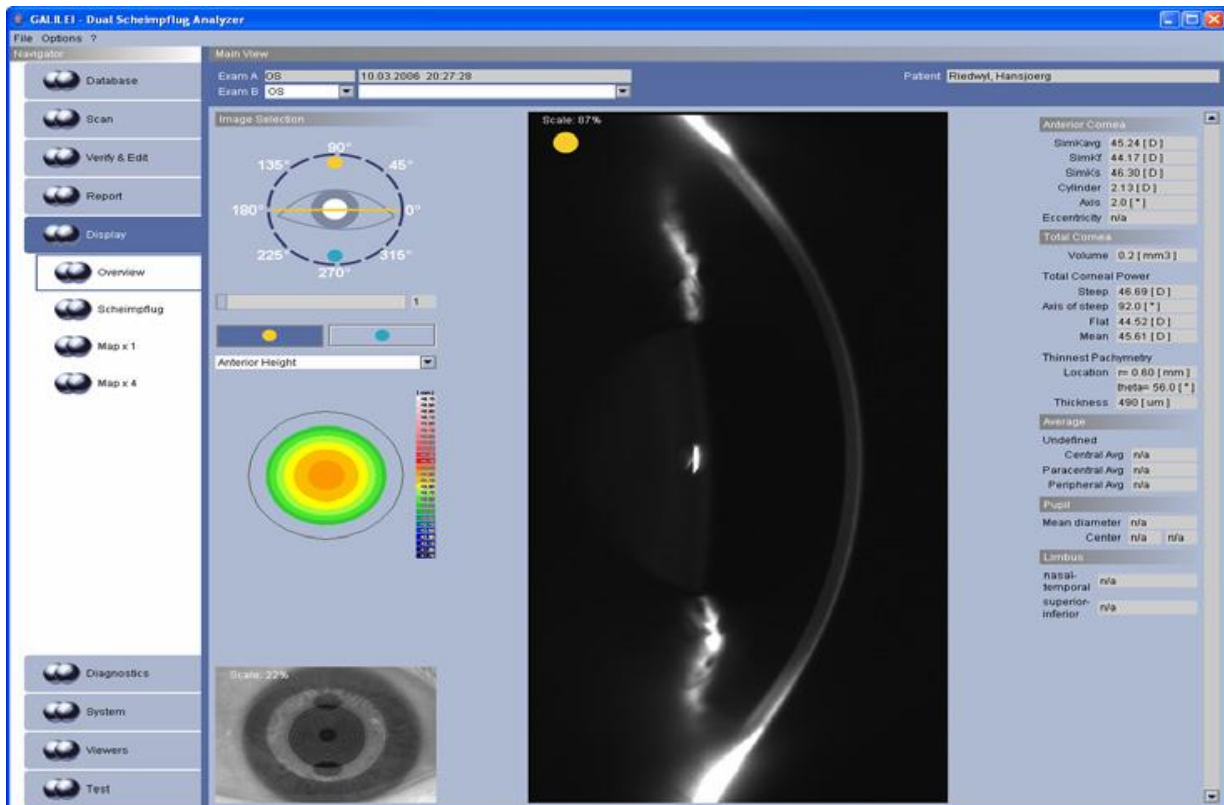


Fig.32a: Screen shot of slit in horizontal position, with simultaneous Placido acquisition in lower left corner, with the orientation shown by the schematic eye diagram in the upper left corner. The Scheimpflug view displayed can be determined by the color of the dot in the corner of the image, on the schematic eye, and on the toggle switch below the schematic eye. In this case, the dot is orange and the slit is aligned horizontally, both of which correspond to the view from the camera in the superior position on the schematic eye. To view the image acquired from the inferior position, the toggle with a blue dot would be chosen.

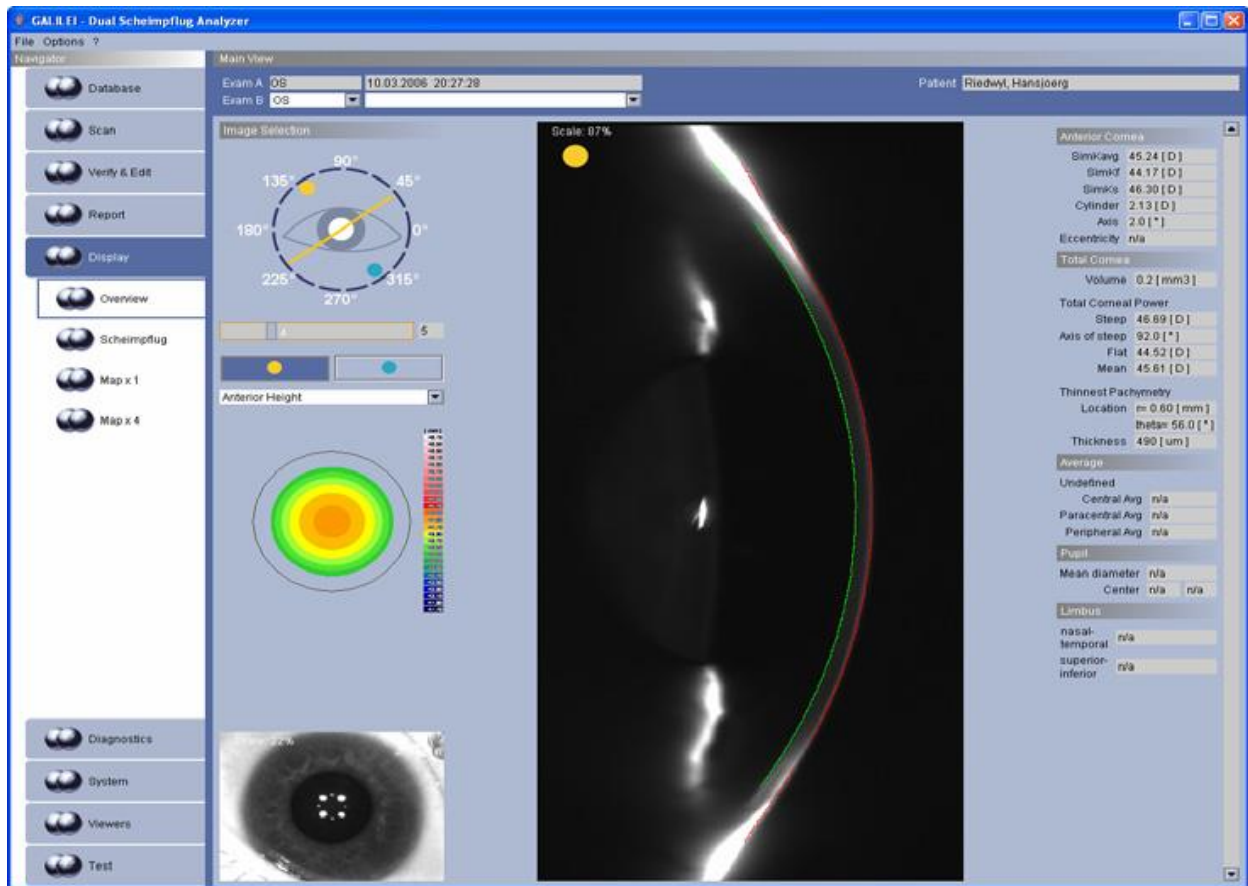


Fig.32b: Screen shot of slit in oblique position, with simultaneous top view in lower left corner.

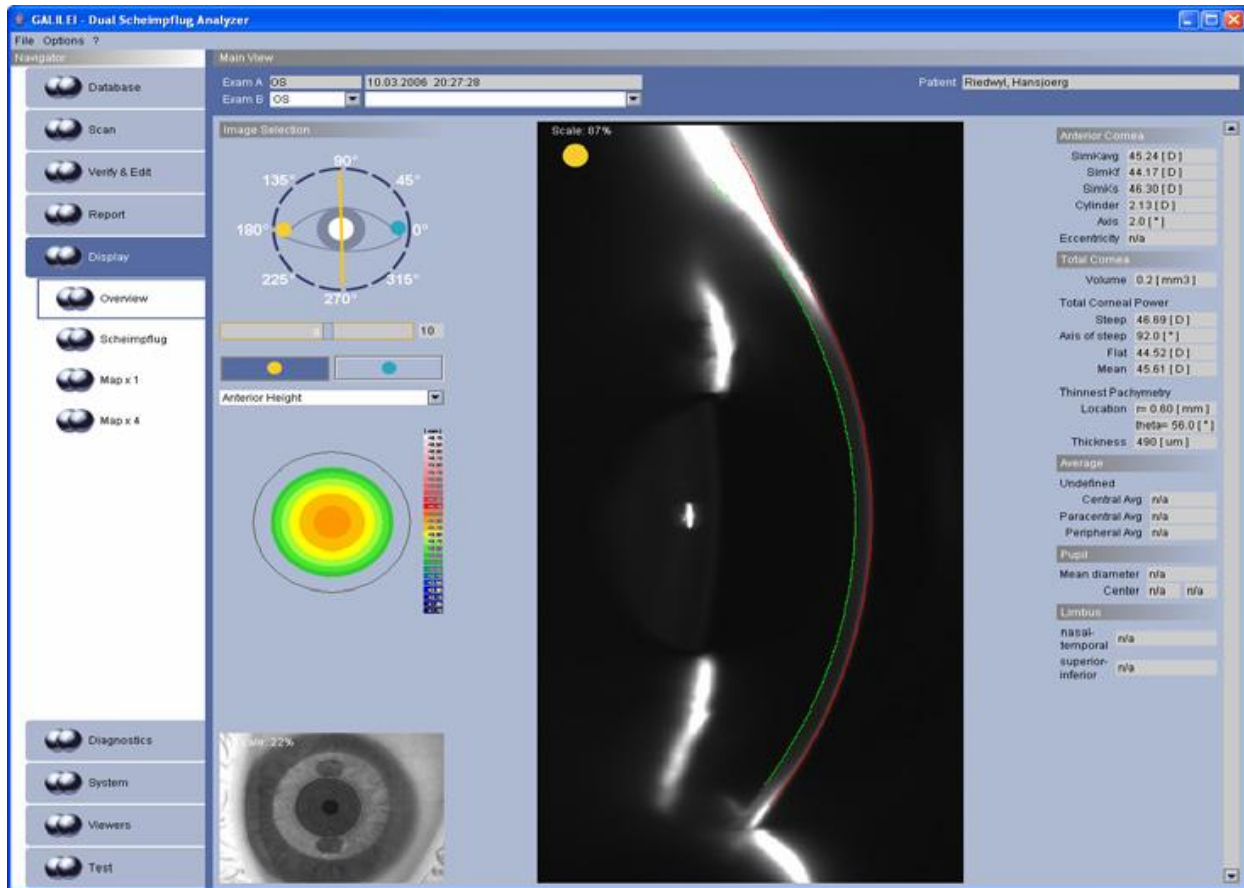


Fig.32c: Screen shot of slit in vertical position, with simultaneous Placido acquisition in lower left corner

3.4.4 Advantages of the GALILEI™ System's Dual Scheimpflug Imaging

In summary, the advantages of the GALILEI™ System's Dual Scheimpflug Imaging with integrated Placido topography include:

1. Direct measurement of anterior corneal surface curvature
2. Direct measurement of elevation of all anterior segment structures
3. Pachymetry calculation that is insensitive to decentration
4. Motion correction from top view camera, in place for Placido capture
5. Greater coverage area in combining both technologies
6. Same reference axis for both technologies.

PART 3

4) Statistical Analysis

For the statistical analysis we used two statistical packages. For simple descriptive statistics we used Excel 2010 (Microsoft Corporation, USA). For further analysis, such as correlations, normality tests, non-parametric tests, graphs and distributions we used the statistical package IBM SPSS Statistics 20 (IBM Corporation, USA).

4.1 First part

The first part of the analysis contains data from 31 keratoconic patients, men and women aged 16-48 from the Vardinoyiannion Eye Institute of Crete (VEIC) and the University Hospital of Heraklion.

Demographic features of subjects and measurements of axial length, corneal curvature and refractive errors (sphere-cylinder) were taken and recorded.

The eyes of each subject were grouped based on keratoconus progress, in more progressed and less progressed keratoconus. The criteria were the astigmatism and the corneal radius.

The mean age of the subjects is 27.58 years. In less progressed keratoconic eyes(lp), the mean values of sphere(sph) and cylinder(cyl) are -0.72D and -1.79D respectively, while the mean value of corneal radius(CRm) is 7.74mm and of axial length(AL) is 24.35mm.

In more progressed keratoconic eyes(mp), the mean values of sphere(sph) and cylinder(cyl) are -0.61D and -3.73D respectively, while the mean value of corneal radius(CRm) is 7.43mm and of axial length(AL) is 24.35mm. The descriptive statistics of the subjects are presented in the table 2 below.

Descriptive Statistics								
	N	Range	Minimum	Maximum	Mean		Std. Deviation	Variance
	Statistic	Statistic	Statistic	Statistic	Statistic	Std. Error	Statistic	Statistic
age	31	32,00	16,00	48,00	27,5806	1,49103	8,30170	68,918
sph_lp	31	5,75	-3,50	2,25	-,7258	,27272	1,51844	2,306
cyl_lp	31	6,00	-6,00	,00	-1,7984	,29201	1,62586	2,643
CRm_lp	31	1,11	7,22	8,33	7,7413	,04715	,26254	,069
AL_lp	31	5,47	22,29	27,76	24,3568	,18419	1,02554	1,052
sph_mp	31	12,25	-8,25	4,00	-,6129	,48009	2,67304	7,145
cyl_mp	31	8,00	-8,50	-,50	-3,7339	,42327	2,35667	5,554
CRm_mp	31	1,55	6,64	8,19	7,4355	,06139	,34182	,117
AL_mp	31	5,38	22,14	27,52	24,3594	,17944	,99908	,998
Valid N (listwise)	31							

Table 2. Descriptive statistics of the patients

4.1.1 More progressed eyes vs less progressed eyes

4.1.2 Axial length

Fig.33 is the scatter plot between the axial lengths in more and less progressed keratoconic eyes. The graph shows a strong relationship between the two variables ($R^2=0.941$). The boxplots in fig.34 shows a difference in the lower bound of the variance in more and less progressed eyes.

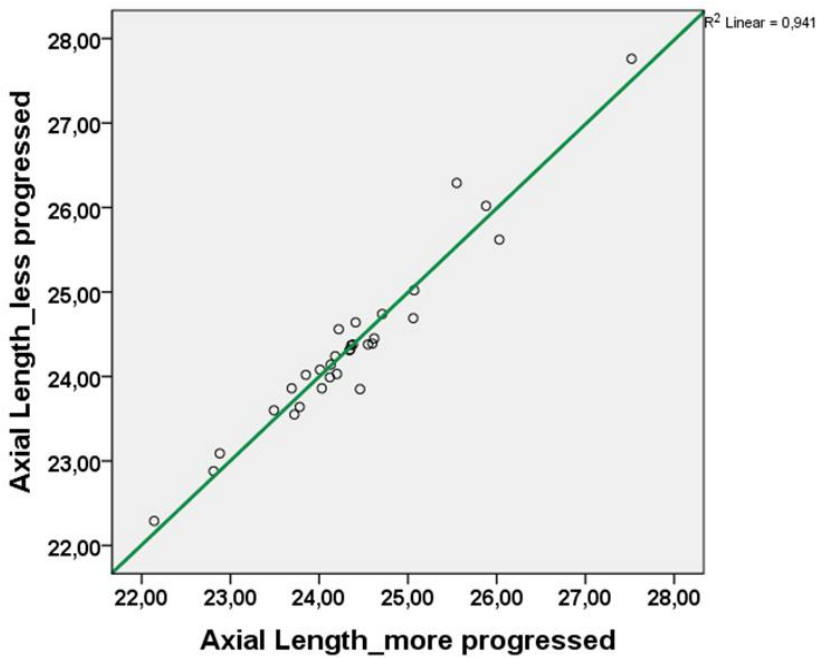


Fig.33 Axial length scatter plot between more and less progressed eyes

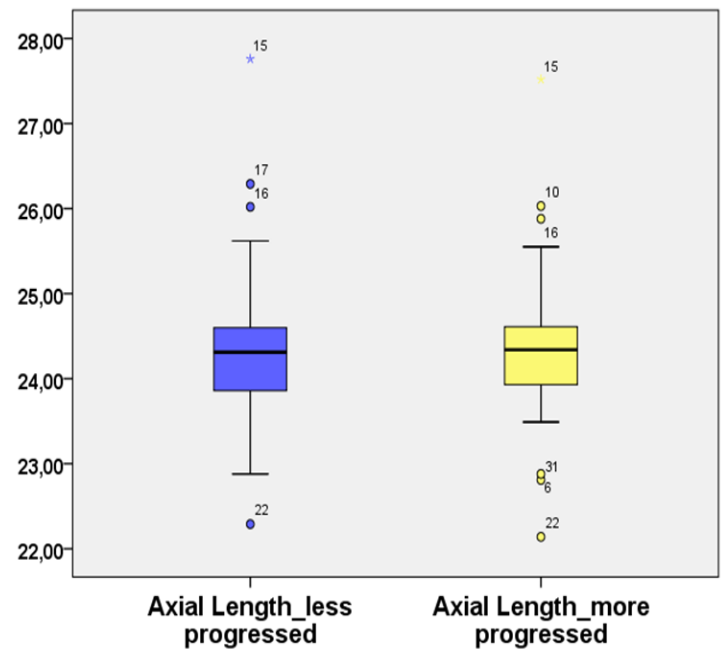


Fig.34 Axial length boxplots between more and less progressed eyes

4.1.3 Corneal Radius

The scatter plot in Fig.35 shows no relationship in corneal radius between more and less progressed eyes.

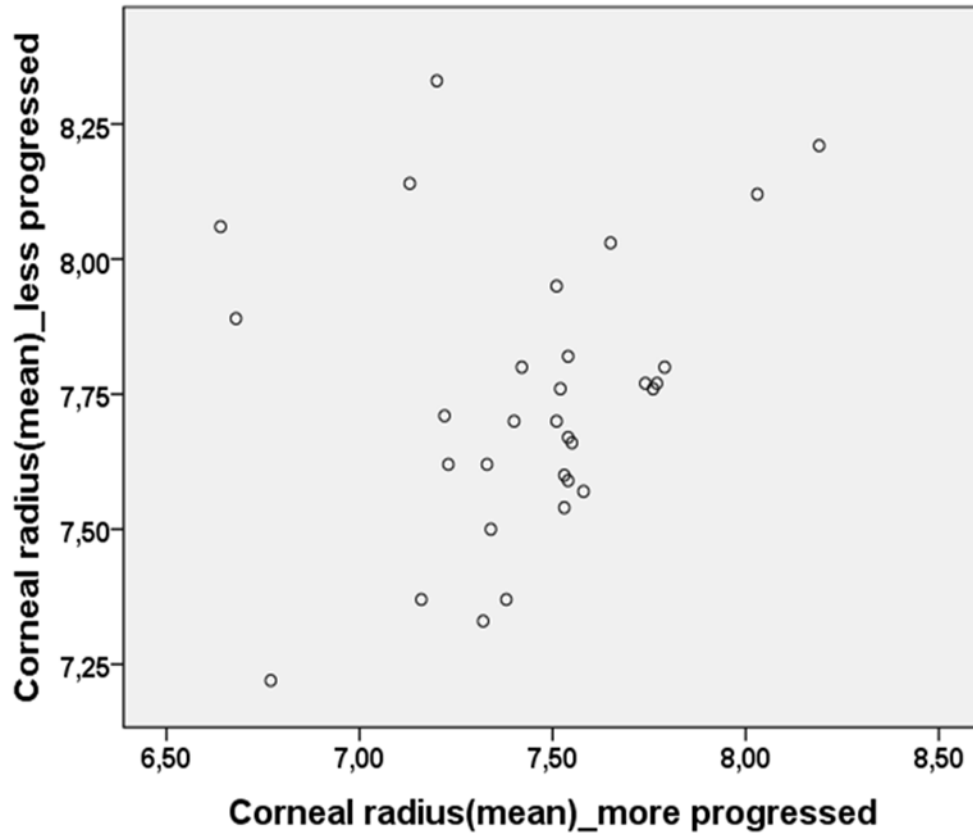


Fig.35 corneal radius' scatter plot between more and less progressed eyes

4.1.4 Axial length vs Corneal radius

Fig.36 shows a strong relationship ($R^2=0.378$) between the axial length and the corneal radius in more and less progressed eyes. This relationship doesn't exist in more progressed eyes (Fig.37.)

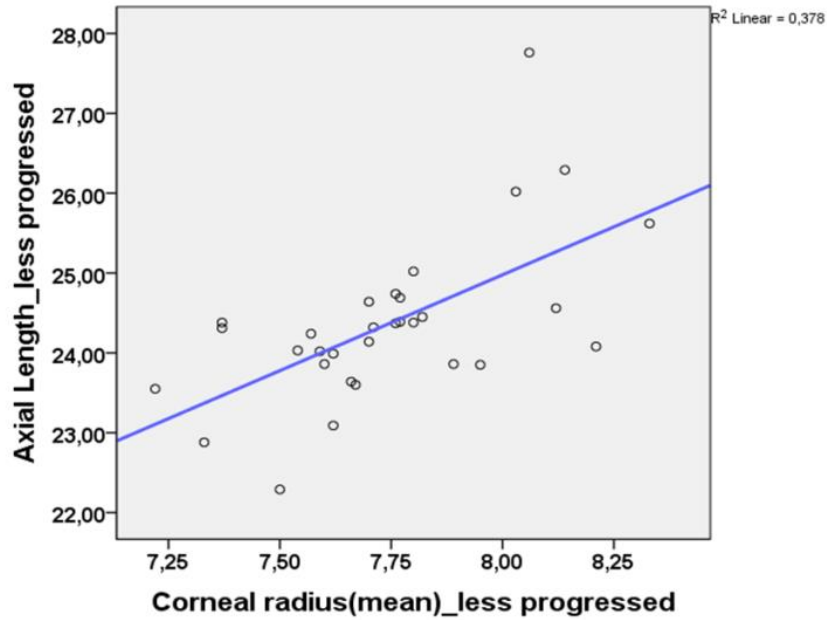


Fig.36 Axial length vs corneal radius scatter plot (less progressed eyes)

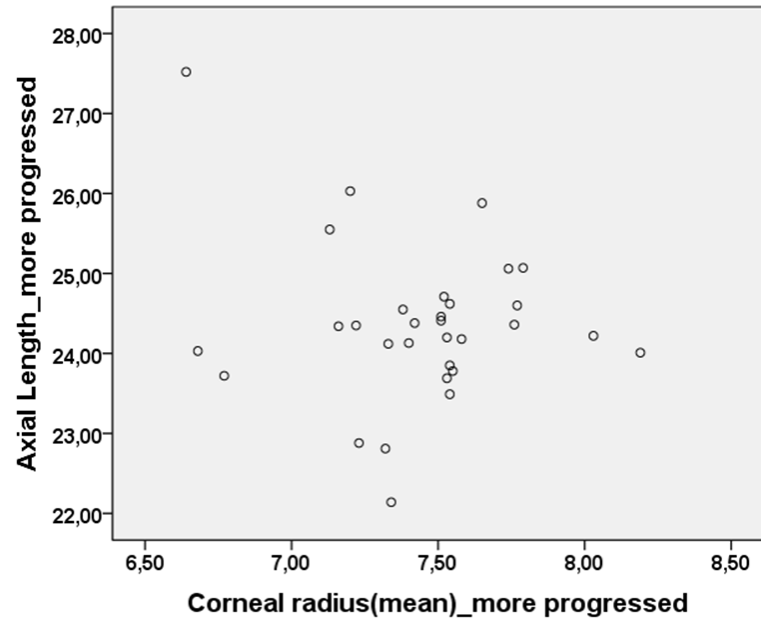


Fig.37 Axial length vs corneal radius scatter plot (more progressed eyes)

4.2 Second part (combined data)

The second part of the analysis contains data collected in another site, by Jos Rozema, University of Antwerpen, Belgium since this is a shared collaborative project.

In this part there are combined data (Greece-Belgium) from 163 keratoconic patients, men and women aged 16-60 years.

Demographic features of subjects and measurements of axial length, corneal curvature and refractive errors (sphere-cylinder) were taken and recorded. The methods for the measurements were the same as the group in the first part of analysis.

The eyes of each subject were grouped based on keratoconus progress, in more progressed and less progressed keratoconus. The criteria were the astigmatism and the corneal radius.

4.2.1 Normality tests

The table 3 below shows the normality coefficients. Our sample contains more than 50 observations, thus the appropriate coefficient is the Kolmogorov-Smirnov.

As we see, in less progressed eyes the variables sphere(sph_lp), cylinder(cyl_lp), corneal radius(CRm_lp), axial length(AL_lp) and corneal radius/axial length (CRm_over_AL_lp) don't follow the Normal distribution. (sig.< 0,05). Only the anterior chamber depth (ACD_lp) variable follows the Normal distribution. (sig.>0, 05)

In more progressed eyes also, the variables sphere(sph_mp), cylinder(cyl_mp), corneal radius(CRm_mp), axial length(AL_mp) and corneal radius/axial length (CRm_over_AL_mp) don't follow the Normal distribution. (sig.< 0,05). Only the anterior chamber depth (ACD_mp) variable follows the Normal distribution. (sig.>0, 05)

	Kolmogorov-Smirnov ^a			Shapiro-Wilk		
	Statistic	df	Sig.	Statistic	df	Sig.
sph_lp	,121	163	,000	,919	163	,000
cyl_lp	,137	163	,000	,908	163	,000
CRm_lp	,072	163	,038	,951	163	,000
AL_lp	,076	163	,022	,977	163	,009
CRm_over_AL_lp	,213	163	,000	,922	163	,000
ACD_lp	,051	163	,200*	,995	163	,886
sph_mp	,140	163	,000	,910	163	,000
cyl_mp	,074	163	,032	,978	163	,011
CRm_mp	,086	163	,005	,972	163	,002
AL_mp	,071	163	,043	,979	163	,015
CRm_over_AL_mp	,160	163	,000	,938	163	,000
ACD_mp	,057	163	,200*	,995	163	,815

*. This is a lower bound of the true significance.

a. Lilliefors Significance Correction

Table 3. normality tests

4.2.2 Distributions

The Fig.38 represents the distributions of axial length, sphere, cylinder, corneal radius, anterior chamber depth and corneal radius/axial length in less progressed eyes.

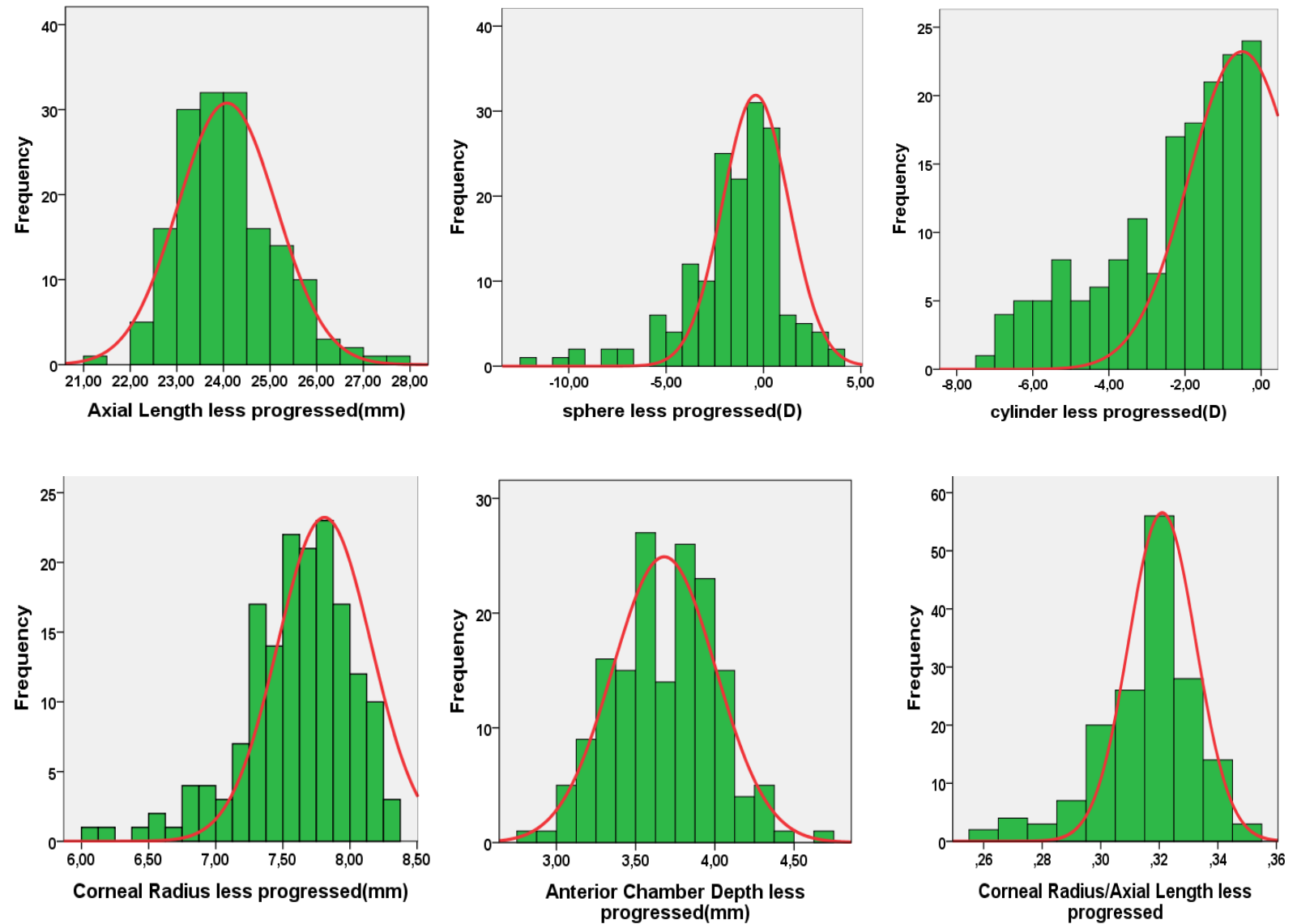


Fig.38 distributions of the variables axial length, sphere, cylinder, corneal radius, anterior chamber depth and corneal radius/axial length in less progressed eyes.

The Fig.39 represents the distributions of axial length, sphere, cylinder, corneal radius, anterior chamber depth and corneal radius/axial length in more progressed eyes.

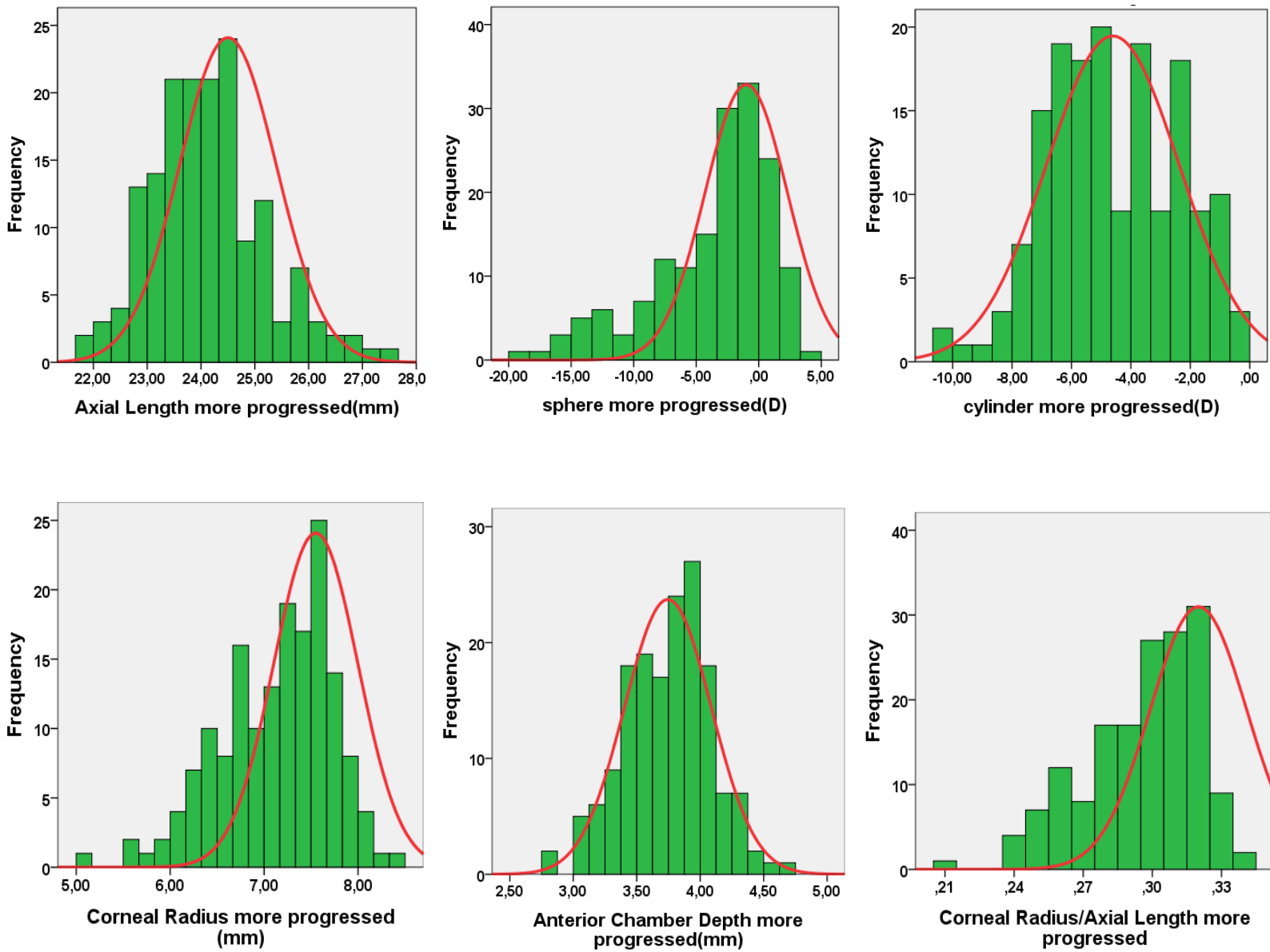


Fig.38 distributions of the variables axial length, sphere, cylinder, corneal radius, anterior chamber depth and corneal radius/axial length in more progressed eyes.

4.2.3 Axial length

The scatter plot in fig.39 shows a strong relationship in axial length between more and less progressed eyes. ($R^2=0.838$).The boxplots in fig.40 show that the variances between the two groups are almost the same. The less progressed eyes have axial length between 21.25mm and 27.76mm, more progressed observations between 21.70mm-27.52mm. The mean values of less- and more progressed keratoconic eyes are 24.08mm and 24.12mm respectively. The difference between the mean values is 0.04mm. Thus, the axial length is almost the same.

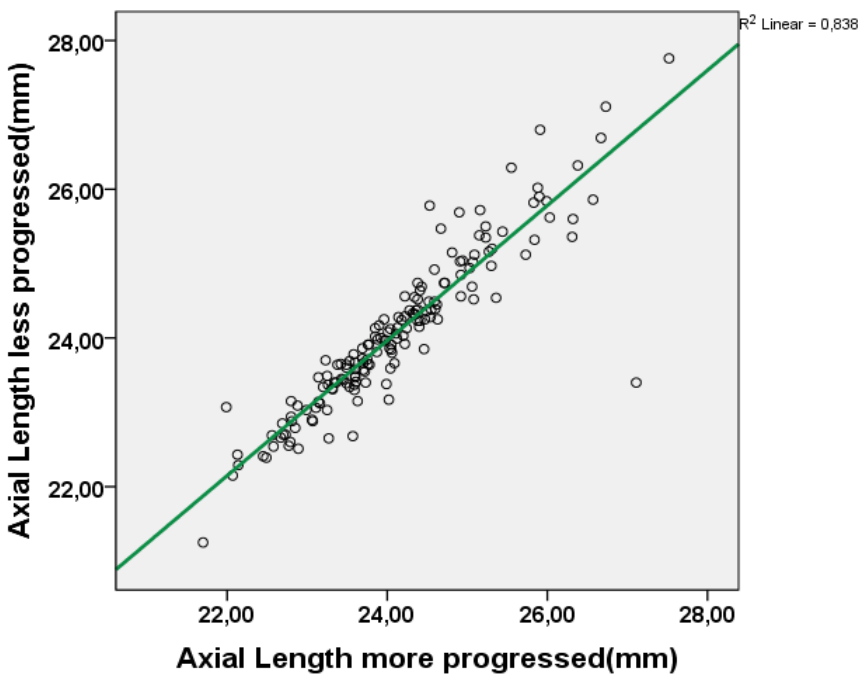


Fig.39 Axial length's scatter plot(less progressed eyes vs more progressed eyes)

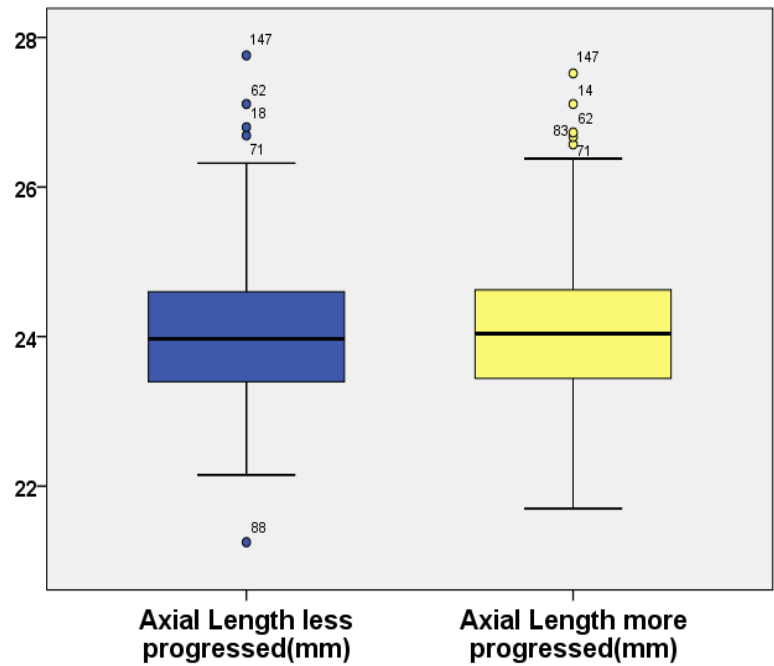


Fig.40 Axial length's boxplots(less progressed eyes vs more progressed eyes)

4.2.4 Sphere

The scatter plot in fig.41 shows a strong relationship in sphere between more and less progressed eyes. ($R^2=0.205$).The boxplots in fig.42 show that the variances between the two groups are different to the lower bound.

The range in less progressed eyes is -11.754D to 4.00D and in more progressed eyes is -19.00D to 4.00D. The mean values in less- and more progressed eyes are -1.54D and -3.58D respectively.

The difference of -2.04D exist because of the ectasia due to the keratoconus, and this is proved by the existence of a significant correlation (non-parametric test, $\rho=-0.246$, p value=0.002<0.05) between the variables Δsph_more_less and ΔL_more_less . (Table 5) Δsph_more_less defined as the difference between the sphere in more and less progressed eyes, and

ΔL_more_less defined as the difference between the axial length in more and less progressed eyes. Both the variables do not follow the normal distribution. The observations are more than 50, thus the appropriate test is the Kolmogorov-Smirnov test. Both the normality coefficients are lower than 0.05. (Table 4)

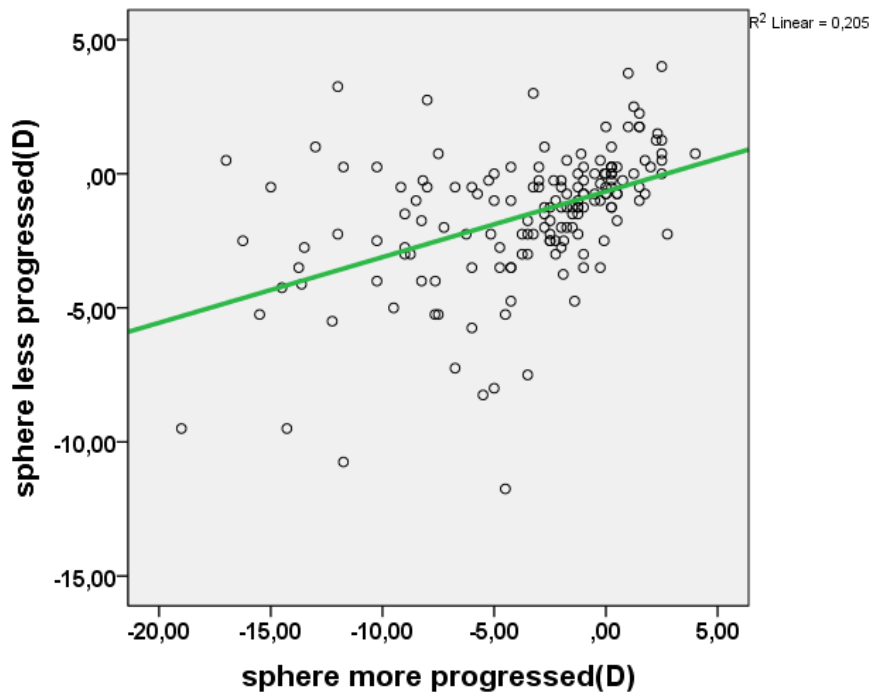


Fig.41 sphere's scatter plot(more vs less progressed eyes)

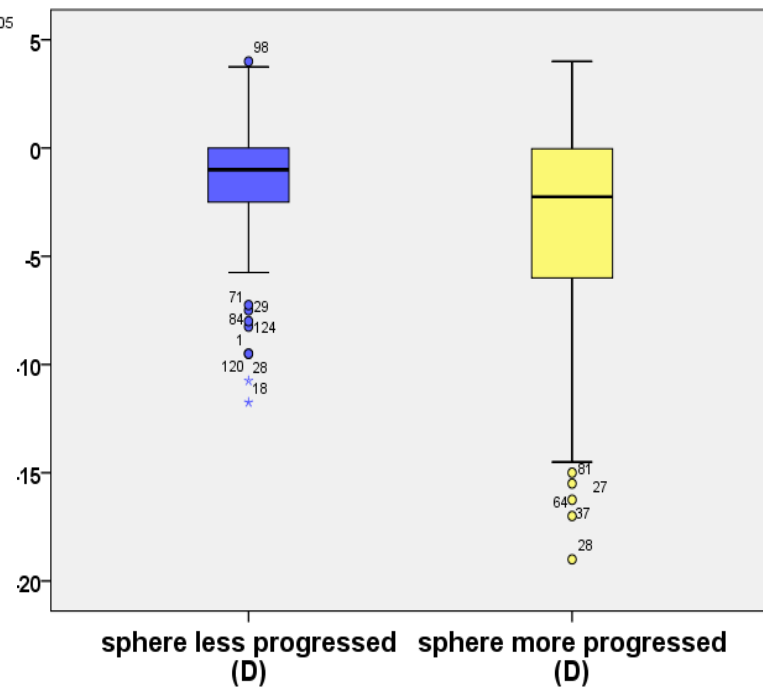


Fig.42 sphere's boxplots(more vs less progressed eyes)

Tests of Normality

	Kolmogorov-Smirnov ^a			Shapiro-Wilk		
	Statistic	df	Sig.	Statistic	df	Sig.
Δ sph_more_less	,183	163	,000	,888	163	,000
Δ L_more_less	,167	163	,000	,736	163	,000

a. Lilliefors Significance Correction

Table 4. Test of normality for the difference between the sphere in more and less progressed eyes and the difference between the axial length in more and less progressed eyes

Correlations

			Δ sph_more_less	Δ L_more_less
Spearman's rho	Δ sph_more_less	Correlation Coefficient	1,000	-,246**
		Sig. (2-tailed)	.	,002
		N	163	163
	Δ L_more_less	Correlation Coefficient	-,246**	1,000
		Sig. (2-tailed)	,002	.
		N	163	163

** . Correlation is significant at the 0.01 level (2-tailed).

Table 5. Correlation(difference between the sphere in more and less progressed eyes vs the difference between the axial length in more and less progressed eyes)

4.2.5 Cylinder

The scatter plot in fig.43 shows a statistical significant relationship in cylinder between more and less progressed eyes. ($R^2=0.146$).The boxplots in fig.44 show that the variances between the two groups differ.

The observations belong between -7.50D to -0.25D (less progressed eyes) and -10.50D to -0.50D (more progressed eyes). The mean values for less and more progressed eyes are -2.50D and -4.50D respectively, and their difference is -2.00D. This difference exists because of the increase in cornea's steepness in more progressed eyes.

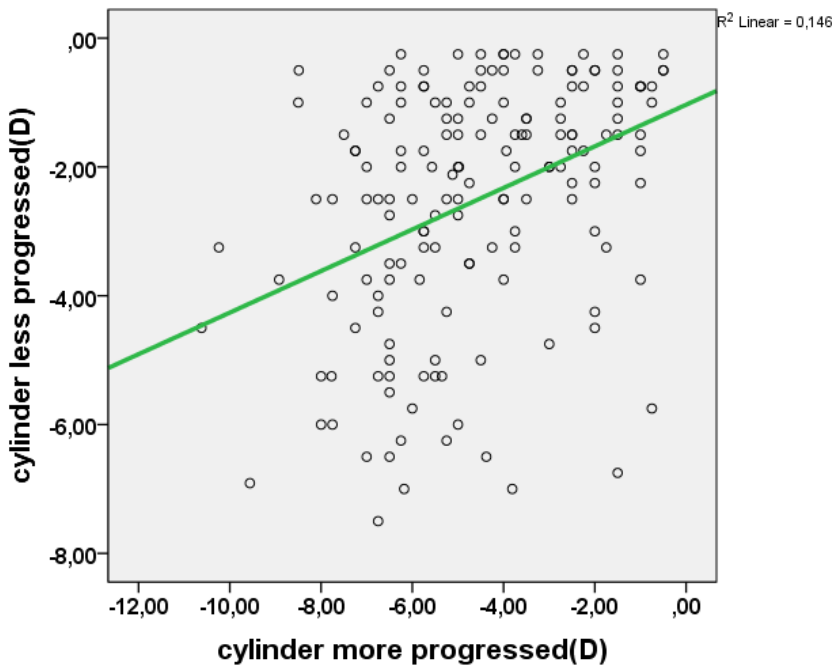


Fig.43 Cylinder's scatter plot (more vs less progressed eyes)

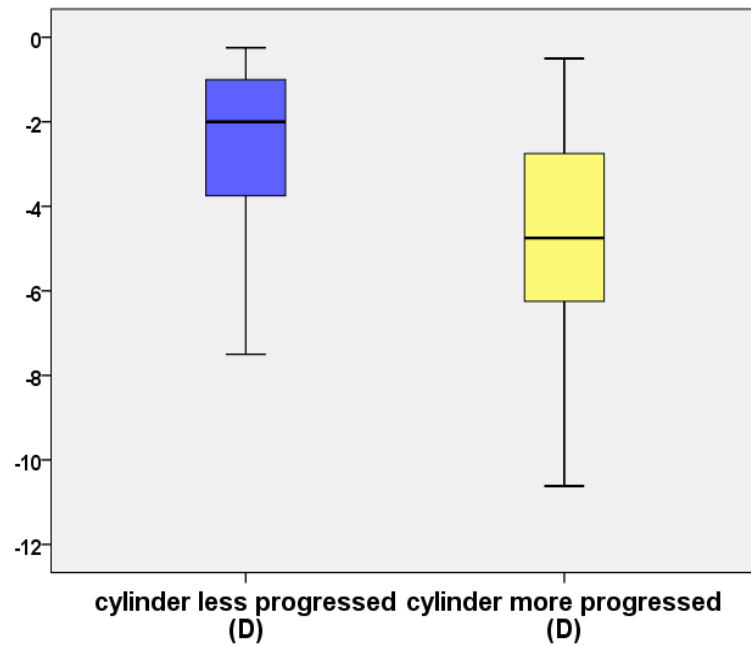


Fig.44 Cylinders boxplots (more vs less progressed eyes)

4.2.6 Corneal radius

The scatter plot in fig.45 shows a strong relationship in corneal radius between more and less progressed eyes. ($R^2=0.393$).The boxplots in fig.46 show that the variances between the two groups differ mostly at the lower bound.

The corneal radius is between 6.80mm-8.40mm in less progressed eyes and 5.97mm-8.28mm in more progressed eyes. The mean value of the corneal radius is 7.60mm and 7.13mm in less- and more progressed eyes respectively. The difference between the means is 0.47mm, thus, the more progressed keratoconic corneas are steeper than the less progressed.

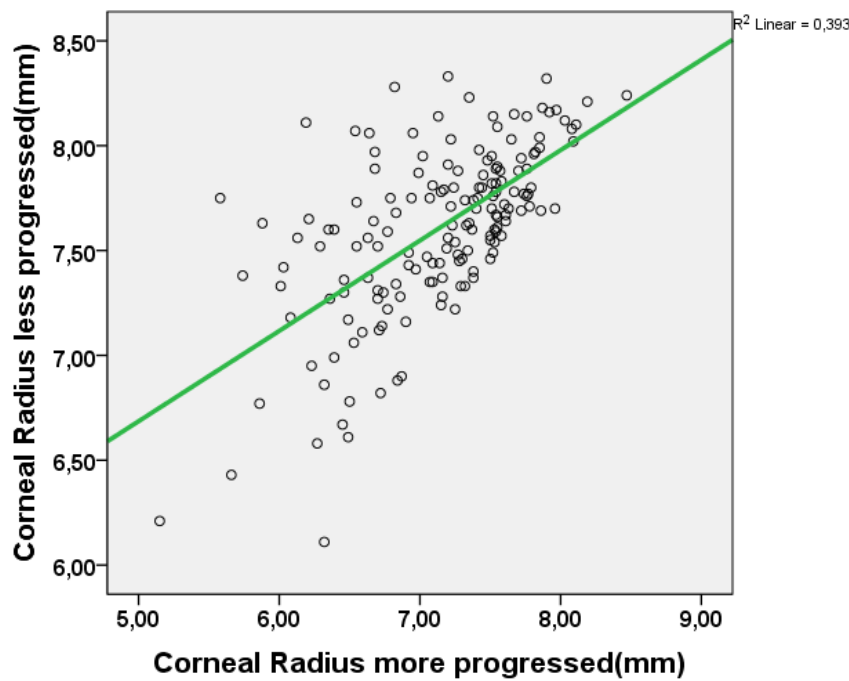


Fig.45 Corneal radius' scatter plot (more vs less progressed eyes)

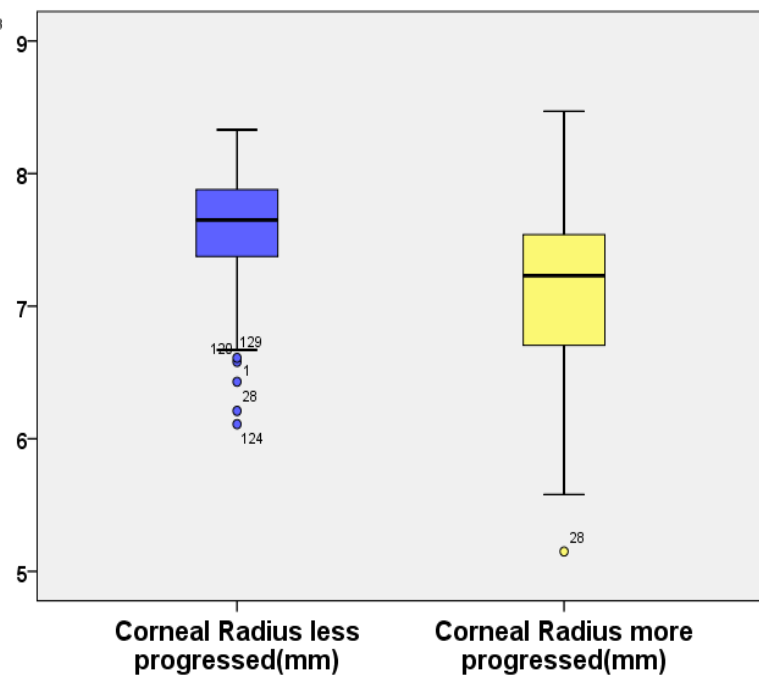


Fig.46 Corneal radius' boxplots (more vs less progressed eyes)

4.2.7 Anterior chamber depth

The scatter plot in fig.47 shows a strong relationship in anterior chamber depth between more and less progressed eyes. ($R^2=0.900$).The boxplots in fig.48 show that the variances between the two groups do not differ significant.

The anterior chamber depth is between 2.87mm-4.67mm in less progressed eyes and 2.81mm-4.65mm in more progressed eyes. The mean value of the anterior chamber depth is 3.68mm and 3.74mm in less- and more progressed eyes respectively. The difference between the means is 0.06mm.

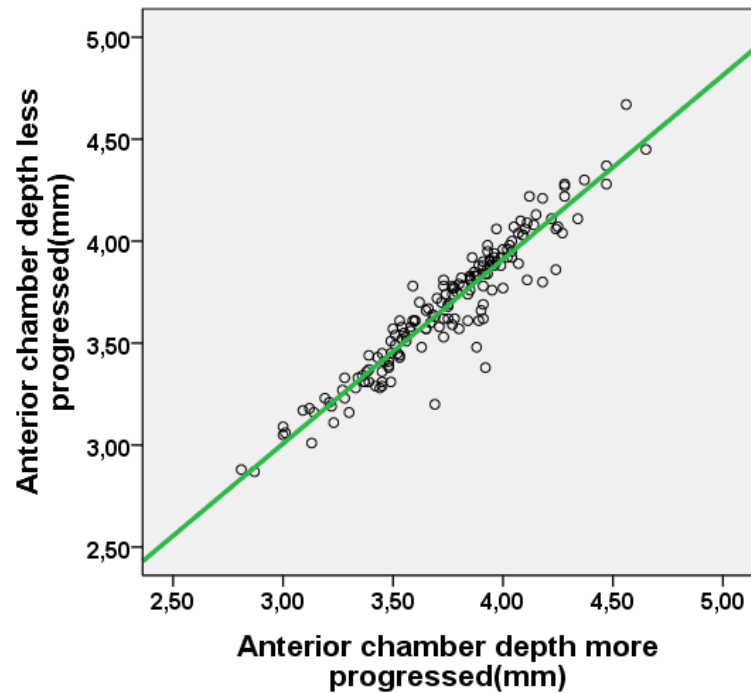


Fig.47 Anterior chamber depth's scatter plot (more vs less progressed eyes)

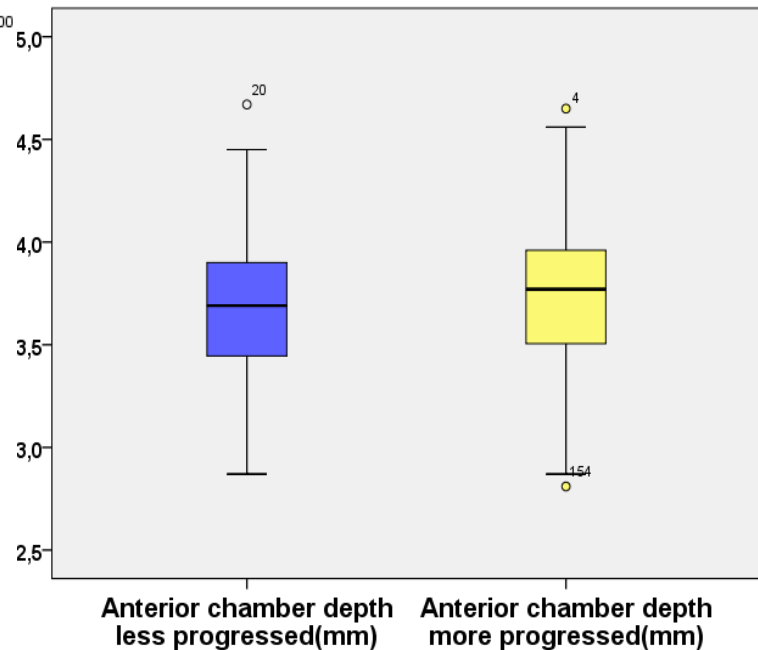


Fig.48 Anterior chamber depth's boxplots (more vs less progressed eyes)

4.2.8 Corneal radius/axial length

The scatter plot in fig.49 shows a strong relationship in corneal radius/axial length between more and less progressed eyes. ($R^2=0.323$).The boxplots in fig.50 show that the variances between the two groups differ at a significant level.

The observations belong between 0.26-0.35 (less progressed eyes) and 0.21-0.34(more progressed eyes). The mean values for less and more progressed eyes are 0.31 and 0.29 respectively, and the difference between the slopes is 0.02.

The less progressed eyes have greater values in corneal radius. Thus, the numerator of the ratio changes, so the whole ratio is affected.

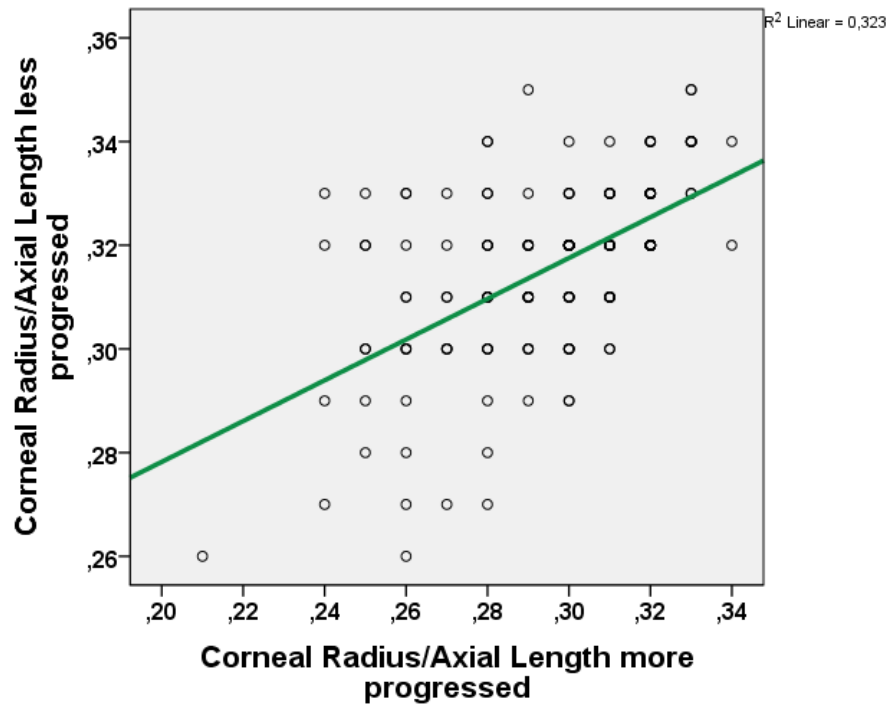


Fig.49 Corneal radius/axial length scatter plot (more vs less progressed eyes)

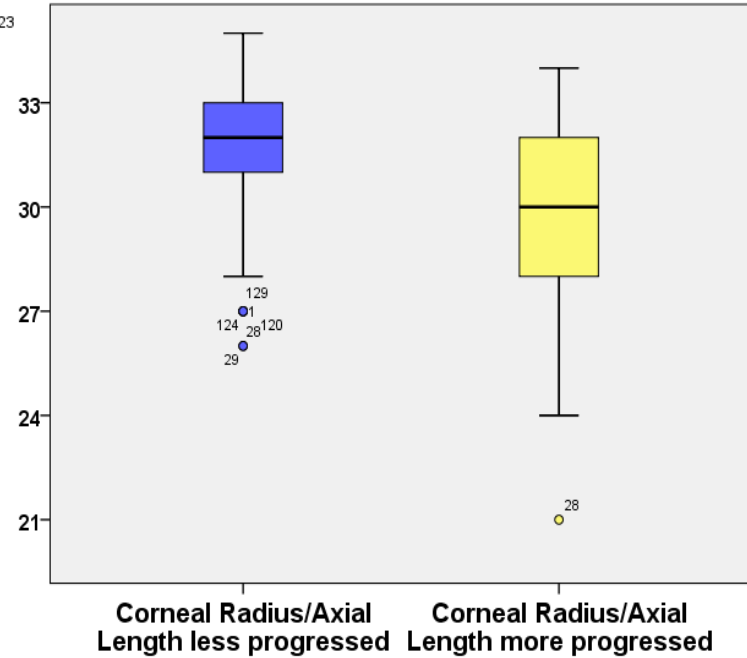


Fig.50 Corneal radius/axial length boxplots (more vs less progressed eyes)

4.2.9 Axial length vs sphere

Fig.51 shows a medium relationship in less progressed eyes between axial length and sphere. ($R^2=0.164$).

This relationship is lost in more progressed eyes. (Fig.52)

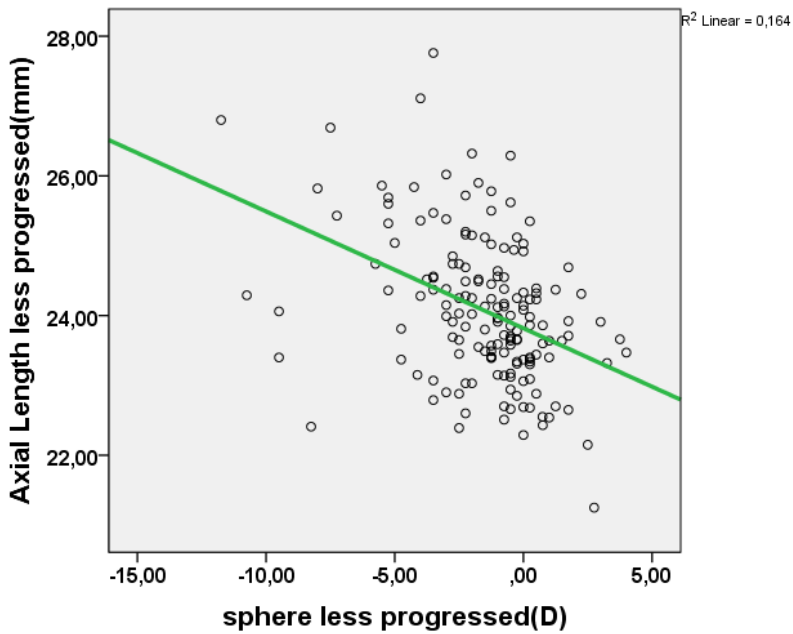


Fig.51 axial length vs sphere scatter plot (less progressed eyes)

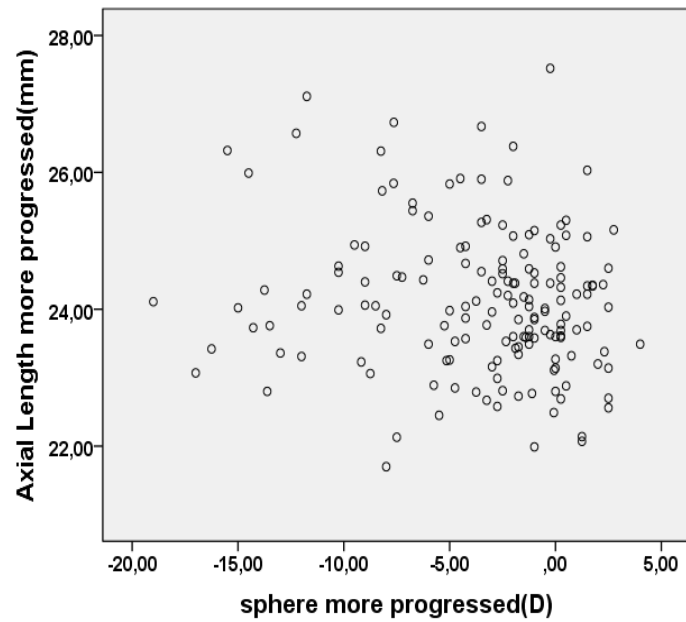


Fig.52 axial length vs sphere scatter plot (more progressed eyes)

4.2.10 Sphere vs Corneal radius

Fig.53 shows the existence of a relationship between sphere and corneal radius in less progressed eyes. ($R^2=0.170$).

This relationship becomes stronger in more progressed eyes. ($R^2=0.485$). As the corneal radius increases so does the sphere. Thus the ectasia because of keratoconus affects myopia.(fig.54)

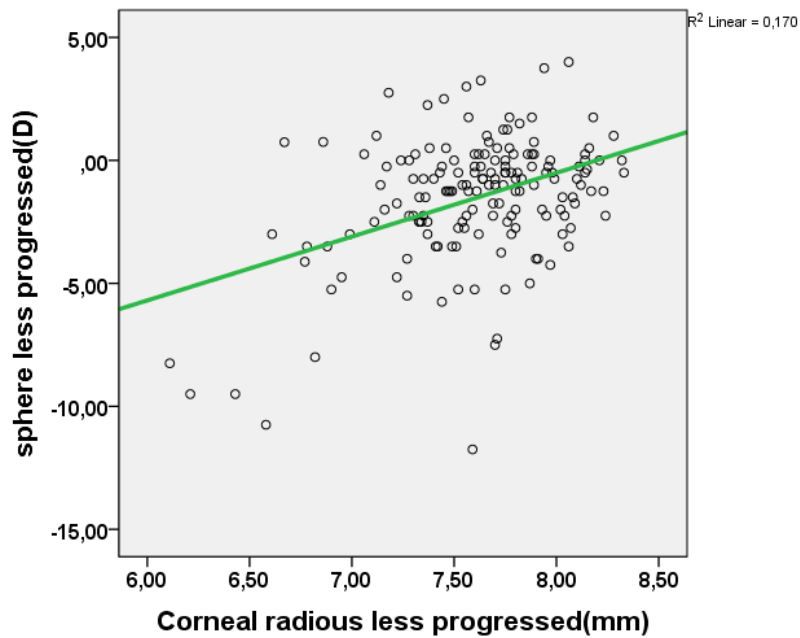


Fig.53 sphere vs corneal radius scatter plot (less progressed eyes)

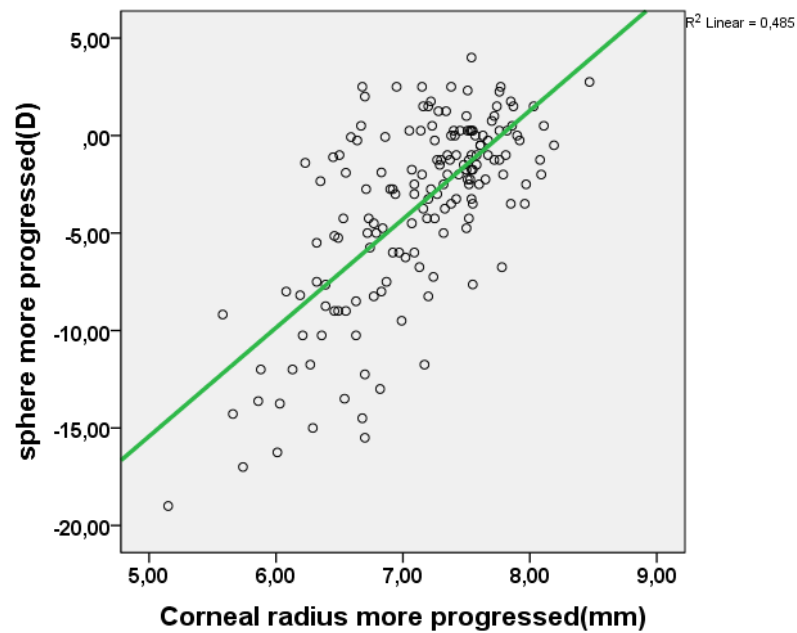


Fig.54 sphere vs corneal radius scatter plot (more progressed eyes)

4.2.11 Axial length vs Anterior chamber depth

The scatter plots in fig.55 and fig.56 show a weak relationship in axial length vs anterior chamber depth between more and less progressed eyes. The relationship is at the same level with $R^2=0.089$ and 0.090 in less and more progressed eyes, respectively.

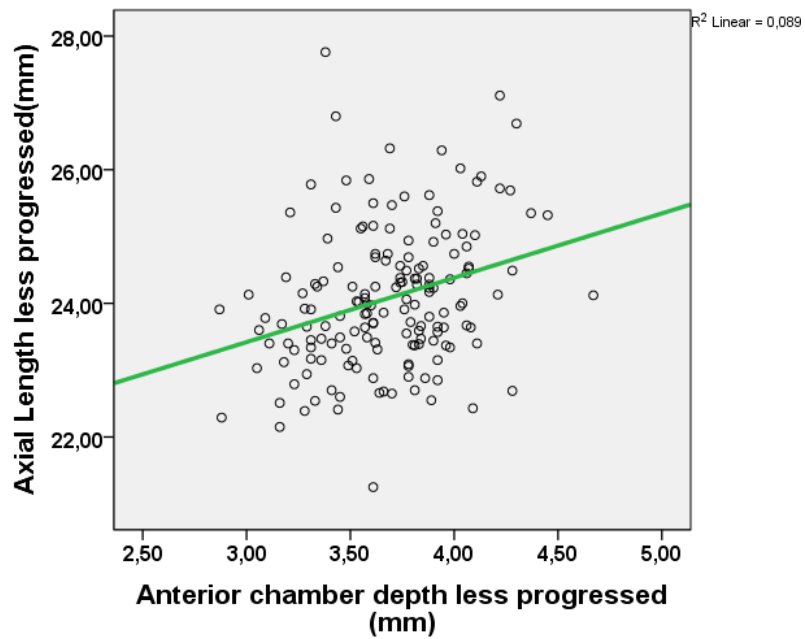


Fig.55 Axial length vs anterior chamber depth scatter plot (less progressed eyes)

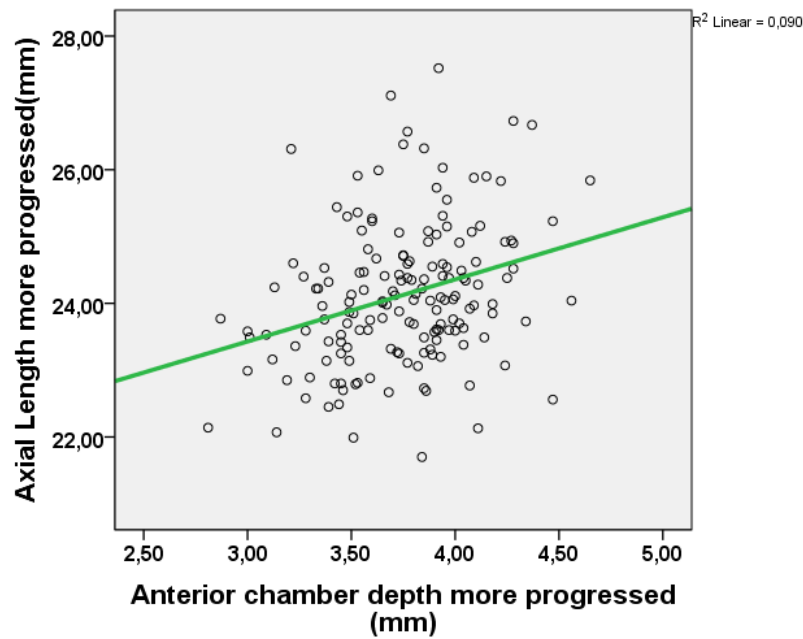


Fig.56 Axial length vs anterior chamber depth scatter plot (more progressed eyes)

4.2.12 Difference in axial length between more and less progressed eyes
(Δ axial length_more_less)

vs

Difference in anterior chamber depth between more and less progressed eyes
(Δ anterior chamber depth_more_less)

Fig.57 shows a medium negative relationship between the variables. ($R^2=0.143$)
Great changes in anterior chamber depth correspond in lower changes in axial length.

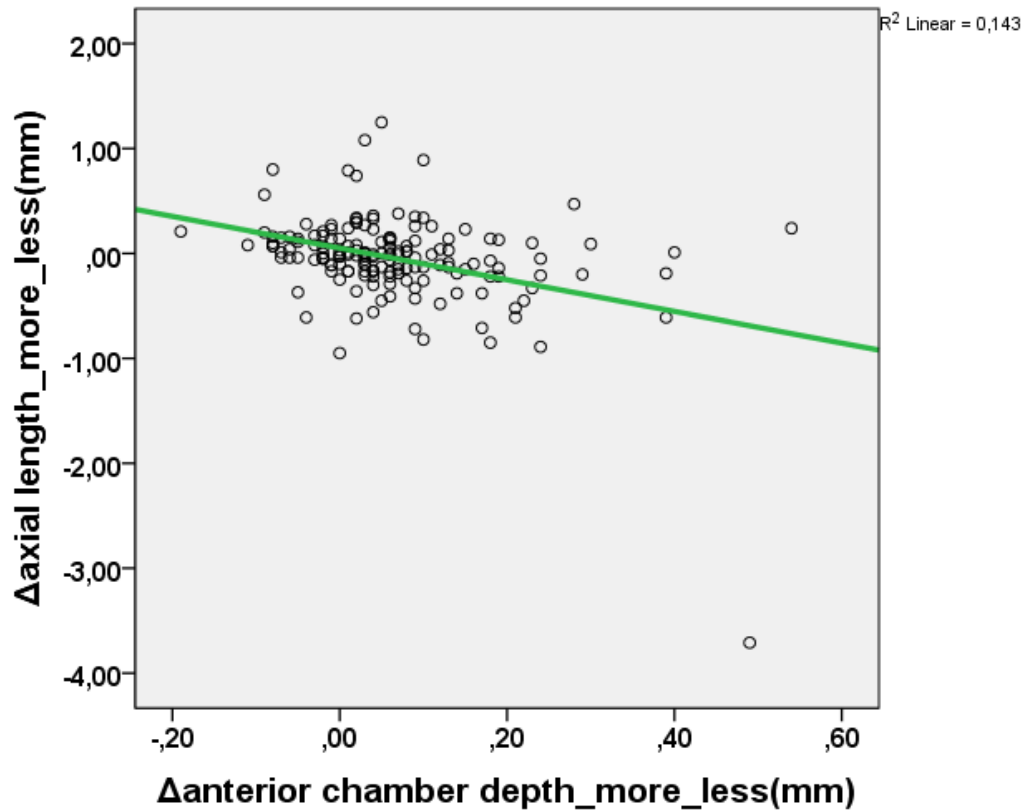


Fig.57 Scatter plot between the differences in axial length and anterior chamber depth(more-less progressed eyes)

4.2.13 Corneal Radius vs Anterior chamber depth

Fig.58 and Fig.59 show that there is no relationship between corneal radius and anterior chamber depth in both groups.

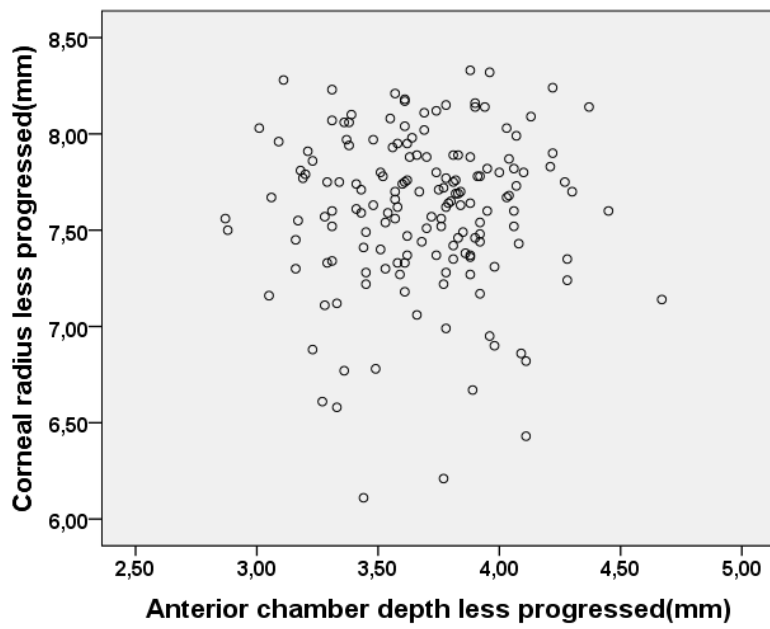


Fig.58 Anterior chamber depth vs corneal radius scatter plot (less progressed eyes)

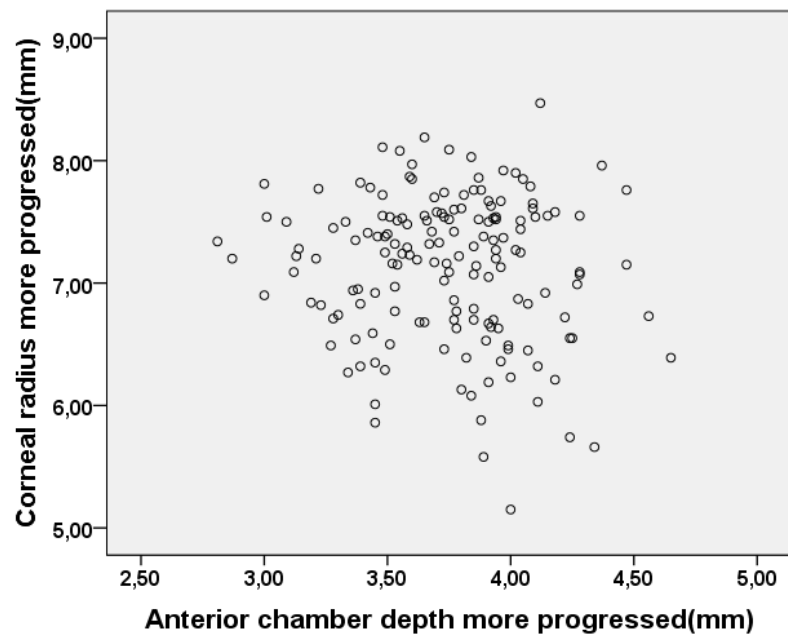


Fig.59 Anterior chamber depth vs corneal radius scatter plot (more progressed eyes)

4.2.14 Difference in corneal radius between more and less progressed eyes
(Δ corneal radius_more_less)

vs

Difference in anterior chamber depth between more and less progressed eyes
(Δ anterior chamber depth_more_less)

Fig.60 shows the existence of a strong negative relationship between the two variables.
($R^2=0.349$).

Great changes in anterior chamber depth correspond in lower changes in corneal radius. Thus, the cone does not affect the measurement of anterior chamber depth.

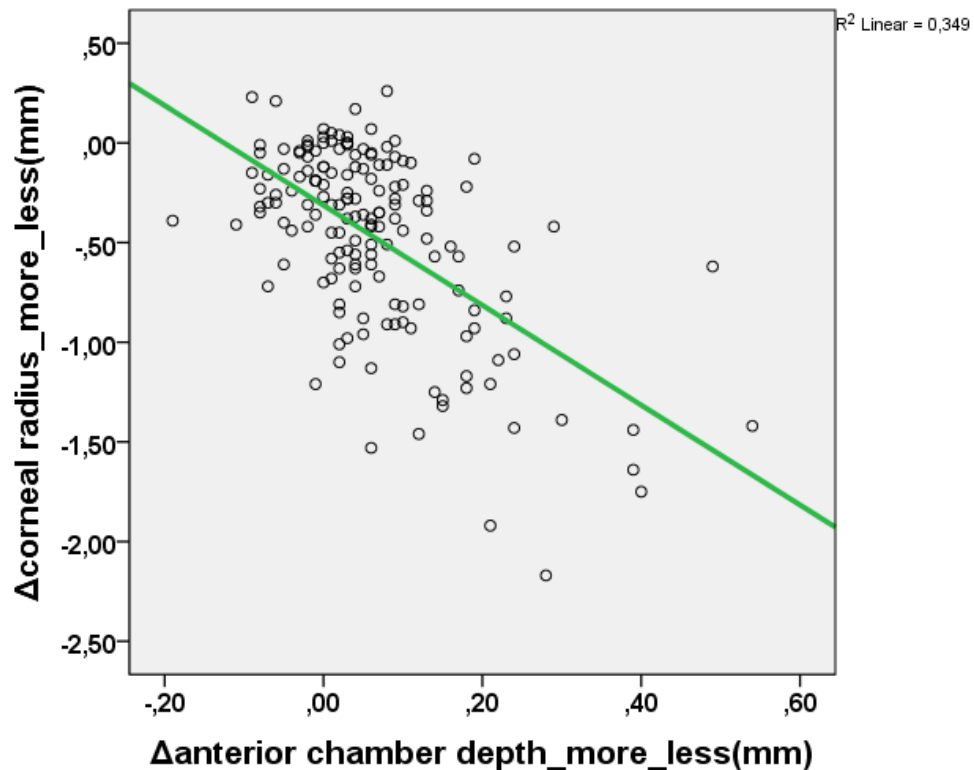


Fig.60 Scatter plot between the differences in corneal radius and anterior chamber depth(more-less progressed eyes)

4.2.15 Corneal radius vs Axial length

Fig.61 shows a medium relationship in less progressed eyes between Corneal Radius-Axial length. ($R^2=0.2017$)

This relationship does not exist in more progressed eyes between Corneal Radius-Axial length.

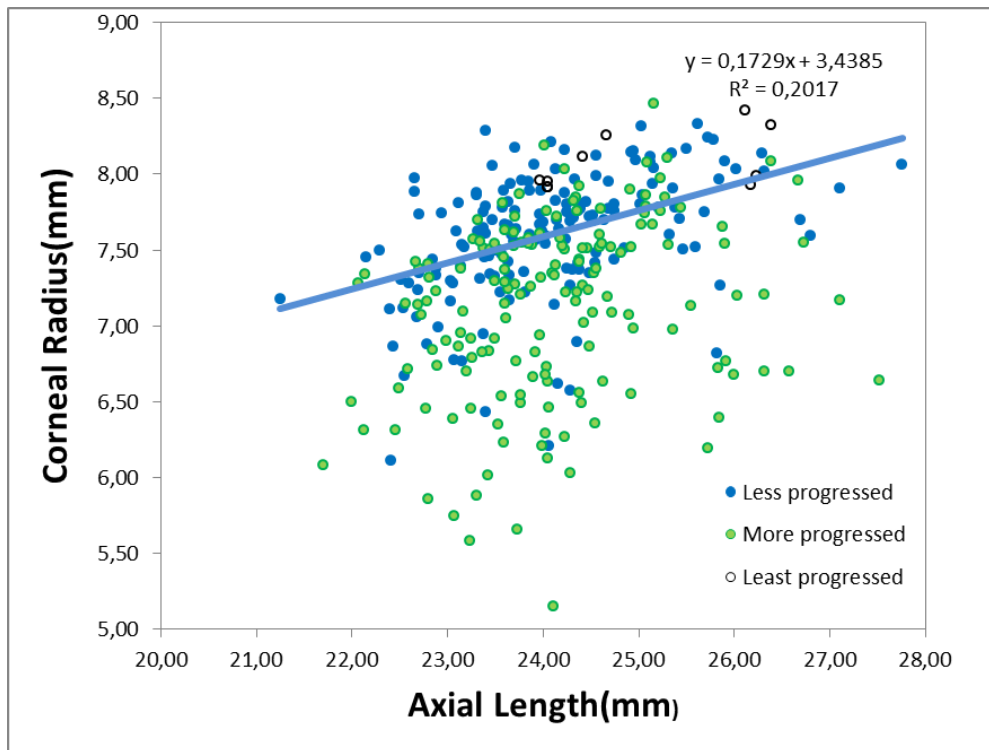


Fig.61 Corneal radius vs Axial length scatter plot(more and less progresses eyes)

5) Discussion

It is important to compare the keratoconic group, with a group of emmetropes. The group of emmetropes which was used is composed by 175 men and women aged 20-40 with a refraction of +0.75D up to -0.74D. The mean age of the group is 30.95 years.

Demographic features of subjects and measurements of axial length, corneal curvature and refractive errors (sphere-cylinder) were taken and recorded. The methods for the measurements were the same as the keratoconic group.

5.1 Normality tests and distributions

Both the variables corneal radius (CRm_emmetropes) and axial length (AL_emmetropes) follow the normal distribution, as the normality coefficients equal both to $0.200 > 0.05$. (Table 6)

Fig. 62 represents the distributions of the variables.

	Kolmogorov-Smirnov ^a			Shapiro-Wilk		
	Statistic	df	Sig.	Statistic	df	Sig.
CRm_emmetropes	,043	175	,200 [*]	,994	175	,641
AL_emmetropes	,038	175	,200 [*]	,988	175	,133

Table 6. normality test for corneal radius and axial length in emmetropes.

*. This is a lower bound of the true significance.

a. Lilliefors Significance Correction

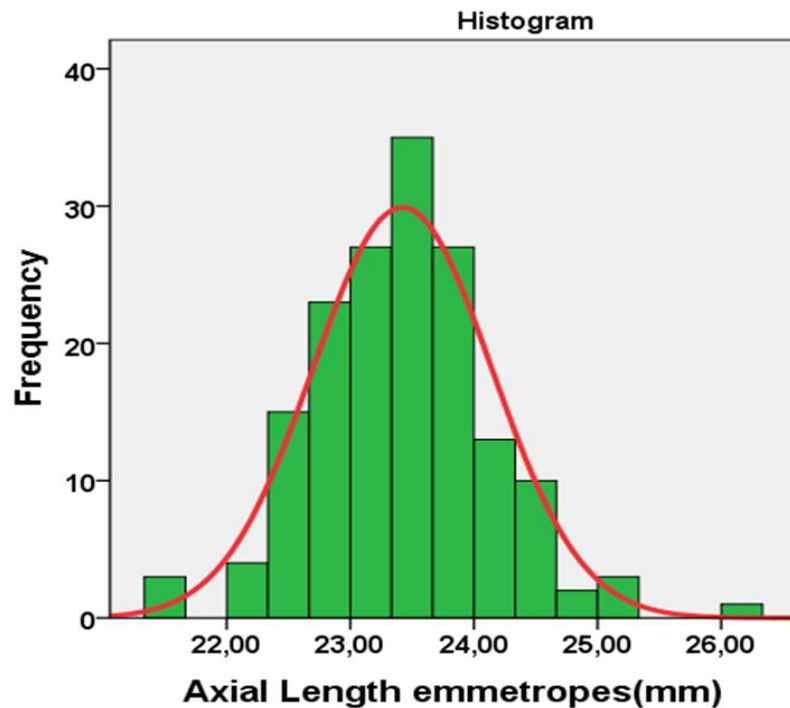
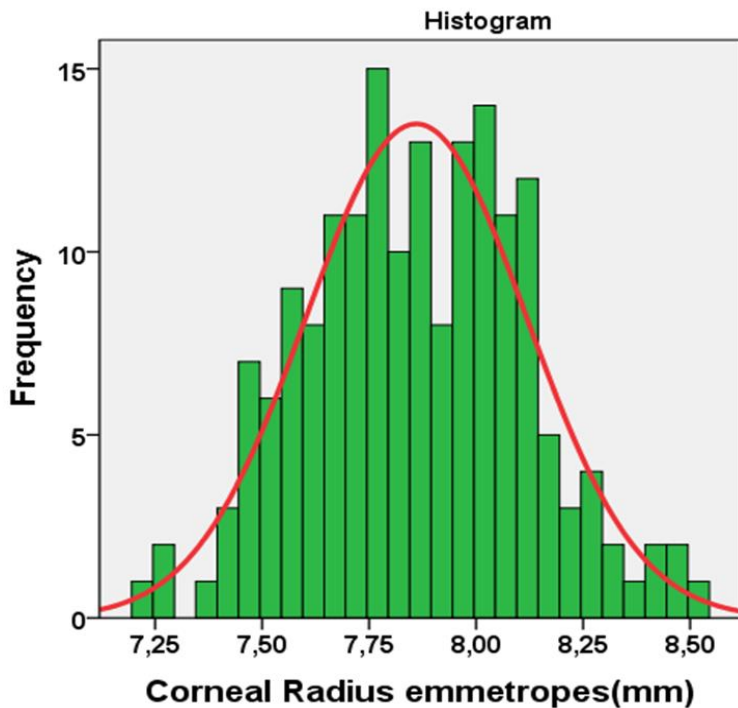


Fig.62 Distributions of corneal radius and axial length(emmetropes)

5.1.2 Axial length

The emmetropic observations have axial length between 22.01mm and 24.84mm, and keratoconic observations (more progressed) between 21.70mm-27.52mm. The mean values of emmetropic and keratoconic eyes are 23.43mm and 24.13mm respectively. The difference between the mean values is 0.70mm and corresponds in a refractive error of approximately 2 D. The keratoconic group is more myopic than the emmetropes (longer eye). The boxplots show a difference in variance's upper bound. Also show that a percentage of keratoconic group is emmetropes, and the rest are myopes.(fig.63)

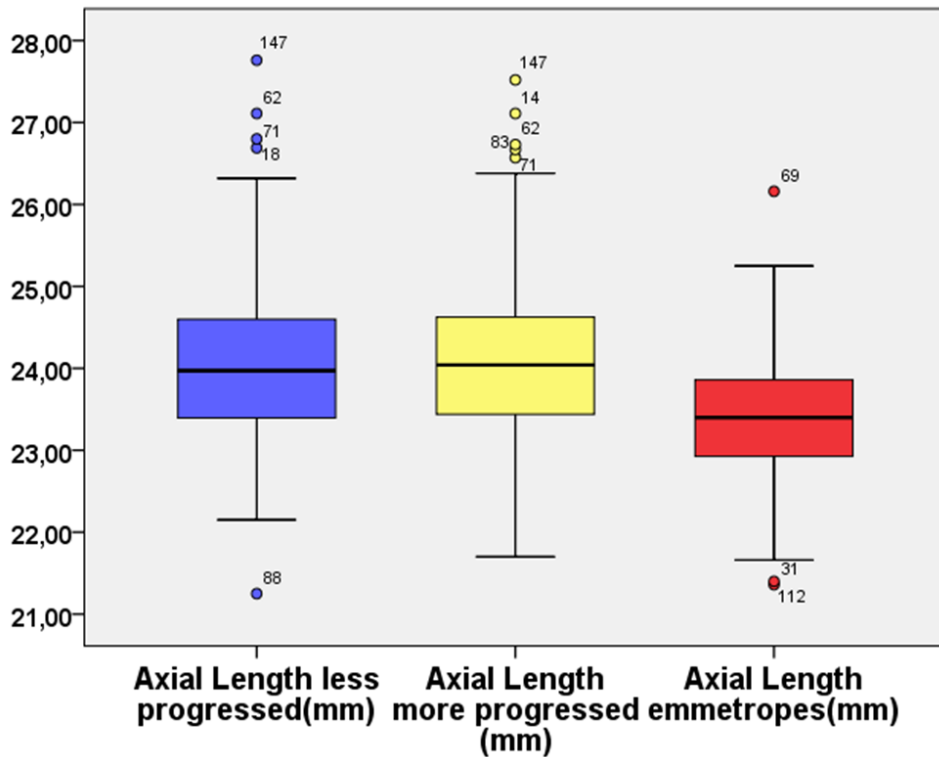


Fig.63 Axial length's boxplots(keratoconic group vs emmetropes)

5.1.3 Corneal radius

The keratoconic group have corneal radius between 5.97mm-8.28mm and the emmetropic group have corneal radius between 7.35mm-8.37mm. The mean values of the corneal radius are 7.13mm and 7.86mm in keratoconic and emmetropic eyes respectively. The difference between the mean values is 0.73mm, thus, the keratoconic corneas are steeper than the emmetropic. The keratoconic group has greater variance than the emmetropic.(fig.64)

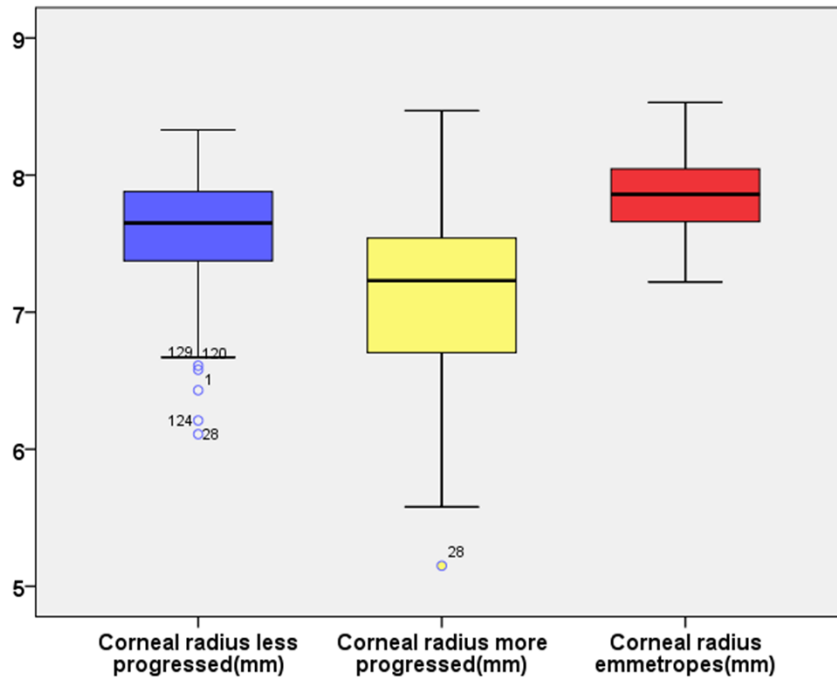


Fig.64 Corneal radius' boxplots(keratoconic group vs emmetropes)

5.1.4 Corneal radius/axial length

The variable CRm_over_AL_emmetropes (corneal radius/axial length in emmetropic group) does not follow the normal distribution. (table 7)

The correlation (non-parametric) is not significant and the p value=0.76>0.05, thus the H₀ (NO correlation between the two variables) is not rejected. (table 8)

The mean values for keratoconic eyes and emmetropes are 0.29 and 0.33 respectively. There is important difference between the slopes in keratoconic eyes and emmetropes despite the fact that the axial length between both groups doesn't differ a lot. The corneal radius in emmetropes follows the Normal distribution, but in keratoconic group doesn't. The emmetropic group has greater values in corneal radius because the emmetropic corneas are flatter than the keratoconic. Thus, the numerator of the ratio changes, so the whole ratio is affected.

Tests of Normality

	Kolmogorov-Smirnov ^a			Shapiro-Wilk		
	Statistic	df	Sig.	Statistic	df	Sig.
CRm_over_AL_emmetropes	,257	175	,000	,872	175	,000

a. Lilliefors Significance Correction

Table 7. Test of normality(corneal radius/axial length in emmetropic group)

Correlations

			CRm_over_AL_mp	CRm_over_AL_emmetropes
Spearman's rho	CRm_over_AL_mp	Correlation Coefficient	1,000	-,023
		Sig. (2-tailed)	.	,767
		N	163	163
	CRm_over_AL_emmetropes	Correlation Coefficient	-,023	1,000
		Sig. (2-tailed)	,767	.
		N	163	175

Table 8. Keratoconic eyes vs emmetropic eyes-correlation of corneal radius/axial length

5.2 Conclusion

Keratoconus is a degenerative eye disorder characterized by thinning and ectasia of the cornea, and causes myopia (ectasia) and abnormal astigmatism. Keratoconus can cause substantial deterioration in patient's vision. Shape, location and dimensions of the cone have major role in vision influence by keratoconus. Keratoconic eyes have steeper corneas, thus, the refraction is affected by the progression of keratoconus. The axial length though, is not affected. The clarification of topographic, biometric and refractive criteria of keratoconus can significantly contribute to the assessment of the development risk factor of keratoconus, the early diagnosis and the effective treatment of the disease.

REFERENCES

1. John T. Siegwart, Jr., Thomas T. Norton, Perspective: How Might Emmetropization and Genetic Factors Produce Myopia in Normal Eyes? *Optom Vis Sci.* 2011 Mar; 88(3): E365–E372.
2. Gilmartin B. Myopia: precedents for research in the twenty-first century. *Clinical and Experimental Ophthalmology.* 2004;32: 305–324.
3. Charman WN. Myopia, posture and the visual environment. *Ophthalmic Physiol Opt.* 2011;31(5):494-501.
4. Fan DS, Cheung EY, Lai RY, Kwok AK, Lam DS. Myopia progression among preschool Chinese children in Hong Kong. *Ann Acad Med Singapore.* 2004;33: 39-43.
5. Dunaway D, Berger I. "Worldwide Distribution of Visual Refractive Errors and What to Expect at a Particular Location".
6. Verma A, Singh D. "Myopia, Phakic IOL." *eMedicine.com.* 19 August 2005.
7. Fredrick DR (May 2002). "Myopia". *BMJ* 324 (7347): 1195–9.
8. National Research Council Commission (1989). *Myopia: Prevalence and Progression*, Washington, D.C. : National Academy Press, ISBN 0-309-04081-7
9. Jensen, A.R. (1998) *The g Factor*. Westport, Connecticut: Praeger Publishers
10. Sperduto RD, Seigel D, Roberts J, Rowland M; Seigel; Roberts; Rowland (1983). "Prevalence of myopia in the United States". *Arch. Ophthalmol.* 101 (3): 405–7.
11. "Discovery of Gene May Provide Treatment for Near-sightedness". *Disabled-world.com.* 12 September 2010. Retrieved 2 August 2012.
12. Chandran S (1972). "Comparative study of refractive errors in West Malaysia". *The British journal of ophthalmology* 56 (6): 492–495
13. Mallen EA, Gammoh Y, Al-Bdour M, Sayegh FN; Gammoh; Al-Bdour; Sayegh (2005). "Refractive error and ocular biometry in Jordanian adults". *Ophthalmic Physiol Opt* 25 (4): 302–9.

14. Mavracanas TA, Mandalos A, Peios D, Golias V, Megalou K, Gregoriadou A, Delidou K, Katsougiannopoulos B; Mandalos; Peios; Golias; Megalou; Gregoriadou; Delidou; Katsougiannopoulos (2000). "Prevalence of myopia in a sample of Greek students". *Acta Ophthalmol Scand* 78 (6): 656–9.
15. Mohan M, Pakrasi S, Zutshi R; Pakrasi; Zutshi (1988). "Myopia in India". *Acta Ophthalmol Suppl* 185: 19–23.
16. Logan NS, Davies LN, Mallen EA, Gilmartin B; Davies; Mallen; Gilmartin (April 2005). "Ametropia and ocular biometry in a U.K. university student population". *Optom Vis Sci* 82 (4): 261–6.
17. Kempen JH, Mitchell P, Lee KE, Tielsch JM, Broman AT, Taylor HR, Ikram MK, Congdon NG, O'Colmain BJ; Mitchell; Lee; Tielsch; Broman; Taylor; Ikram; Congdon; O'Colmain; Eye Diseases Prevalence Research Group (2004). "The prevalence of refractive errors among adults in the United States, Western Europe, and Australia". *Arch. Ophthalmol.* 122 (4): 495–505
18. Vitale S, Sperduto RD, Ferris FL; Sperduto; Ferris FL (2009). "Increased Prevalence of Myopia in the United States Between 1971–1972 and 1999–2004". *Arch Ophthalmol* 127 (12): 1632–9.
19. Kleinstejn RN, Jones LA, Hullett S, Kwon S, Lee RJ, Friedman NE, Manny RE, Mutti DO, Yu JA, Zadnik K; Jones; Hullett; Kwon; Lee; Friedman; Manny; Mutti; Yu; Zadnik; Collaborative Longitudinal Evaluation of Ethnicity Refractive Error Study Group (August 2003). "Refractive error and ethnicity in children". *Arch. Ophthalmol.* 121 (8): 1141–7
20. Wensor M, McCarty CA, Taylor HR; McCarty; Taylor (May 1999). "Prevalence and risk factors of myopia in Victoria, Australia". *Arch. Ophthalmol.* 117 (5): 658–63.
21. Junghans BM, Crewther SG; Crewther (2005). "Little evidence for an epidemic of myopia in Australian primary school children over the last 30 years". *BMC Ophthalmol* 5: 1.
22. Thorn F, Cruz AA, Machado AJ, Carvalho RA; Cruz; Machado; Carvalho (April 2005). "Refractive status of indigenous people in the northwestern Amazon region of Brazil". *Optom Vis Sci* 82 (4): 267–72.

23. Garcia CA, Oréface F, Nobre GF, Souza Dde B, Rocha ML, Vianna RN; Oréface; Nobre; Souza Dde; Rocha; Vianna (2005). "[Prevalence of refractive errors in students in Northeastern Brazil.]". *Arq Bras Oftalmol* (in Portuguese) 68 (3): 321–5..
24. *Cornea*, second edition, Part VII, Krachmer Mannis Holland, Elsevier Science Health Science div
25. *External Disease and Cornea*, Section 8. Basic and Clinical Science Course, AAO, 2006.
26. H.E., Barron, L., McDonald, M.B., eds., *The Cornea*, 2d ed., 1996
27. Tan B1, Baker K, Chen YL, Lewis JW, Shi L, Swartz T, Wang M, How keratoconus influences optical performance of the eye. *J Vis.* 2008 Feb 28;8(2):13.1-10. doi: 10.1167/8.12.13.
28. Colin J., Ertan A., eds. *Intracorneal Ring Segments and Alternative Treatments for Corneal Ectatic Diseases*. Kudret Eye Hosital, Kavaklidere-Ankara, Turkey.
29. product page of A.KRÜSS Optronic GmbH (read March 13, 2013)
30. Canon RK_F1 User Manual
31. Zeiss IOL Master User Manual
32. Olsen, T. and M. Thorwest, Calibration of axial length measurements with the Zeiss IOL Master. *J Cataract Refract Surg*, 2005. 31(7): p. 1345-50.
33. Wolffsohn, J.S. and L.N. Davies, Advances in anterior segment imaging. *Curr Opin Ophthalmol*, 2007. 18(1): p. 32-8.
34. Albert Michelson; Edward Morley (1887). "On the Relative Motion of the Earth and the Luminiferous Ether". *American Journal of Science* 34 (203): 333–345
35. Hariharan, P. (2007). *Basics of Interferometry*, Second Edition. Elsevier.
36. Cynthia J. Roberts, Benno J. Züger, *The Advantage and Principle of Dual Scheimpflug Imaging for Analyzing the Anterior Segment of the Human Eye*
37. Galilei Ziemer User manual